Electronic Supplementary Material (ESI) for CrystEngComm.


# Supporting Information

# Metal-organic frameworks with open metal sites act as efficient heterogeneous catalysts for Knoevenagel condensation and Chan-Lam coupling reaction

*Anindita Goswami, Prantik Dutta and Kumar Biradha**

Department of Chemistry, Indian Institute of Technology Kharagpur, 721302 Kharagpur, India E-mail: kbiradha@chem.iitkgp.ernet.in; Fax: +91-3222-282252; Tel: +91-3222-283346.

CCDC Numbers for the crystal structures are CCDC 2278988, 2278989

## Contents:

**<u>Section S8</u>: Comparison Table for Catalytic Activity and Conversion Efficiency of Cd-CDA-MOF and Cu-CDA-MOF with the recently reported MOF catalysts**

## <u>Section S1:</u>

**Table S1.** Pertinent Crystallographic Parameters for **Cd-CDA-MOF** and **Cu-CDA-MOF**

| | **Cd-CDA-MOF** | **Cu-CDA-MOF** |
|---|---|---|
| CCDC Number | 2278988 | 2278989 |
| Formula | $C_{52}H_{84}Cd_3N_6O_{36}$$ | $C_{312}H_{276}Cu_{24}N_{30}O_{144}$$ |
| Mol.Wt. | 1706.45 | 8274.57 |
| T (k) | 300(2) | 120(2) |
| Crystal System | Monoclinic | Tetragonal |
| Space group | C2/c | I4/m |
| a (Å) | 36.833(5) | 30.4107(13) |
| b (Å) | 10.2950(14) | 30.4107(13) |
| c (Å) | 20.105(3) | 30.414 |
| α (˚) | 90 | 90 |
| β (˚) | 102.065(6) | 90 |
| γ (˚) | 90 | 90 |
| V ($Å^3$) | 7455.3(17) | 28127(2) |
| Z | 4 | 2 |
| D ($g/cm^3$) | 1.492 | 1.009 |
| $R_1$[I >2σ(I)] | 0.0896 | 0.0585 |
| $wR_2$(on $F^2$, all data) | 0.2476 | 0.2118 |

$ The structural formulae for Cd-CDA-MOF and Cu-CDA-MOF are ($\{[Cd_2(CDA)_2]\cdot Cd(H_2O)_6\cdot(NH_2Me_2)_2\cdot 10\ H_2O\}_n$) and ($\{[Cu_{24}(CDA)_{12}(H_2O)_{16}(DMA)_8]\cdot(solv.)_x\}_n$ respectively. $(solv)_x$ is disordered DMA and/or $H_2O$

## Section S2: Thermogravimetric Analyses

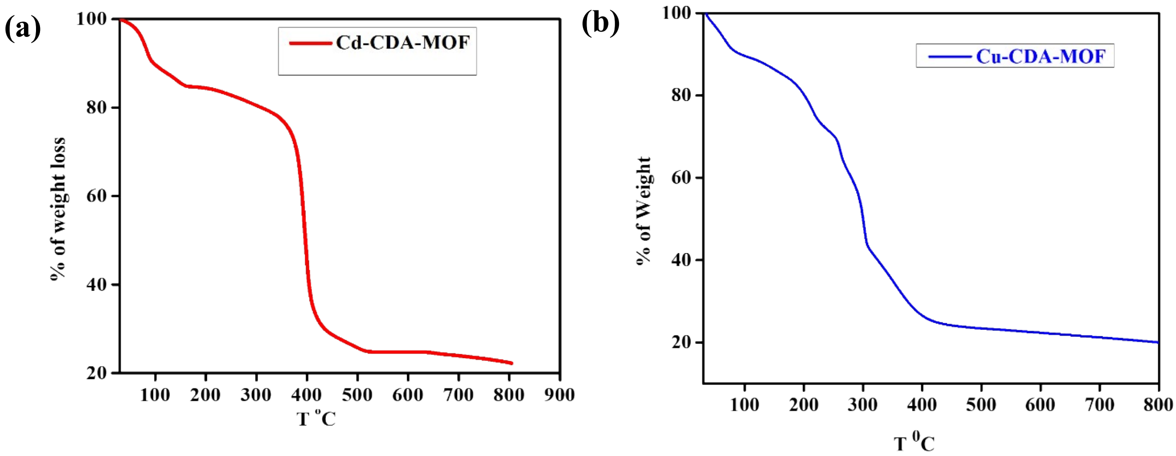


**Figure S1.** Thermogravimetric Analyses: (a) **Cd-CDA-MOF**; (b) **Cu-CDA-MOF**.

## Section S3: FESEM analysis of Cd-CDA-MOF and Cu-CDA-MOF.

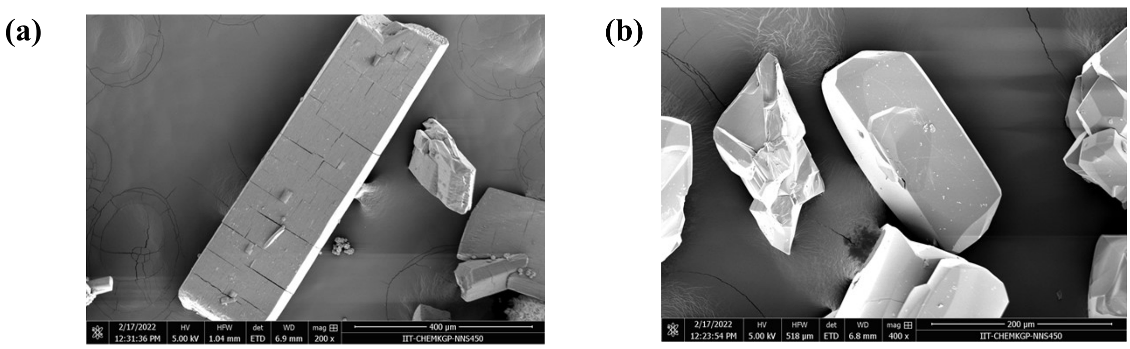


**Figure S2.** FESEM Analyses of (a) **Cd-CDA-MOF**; and (b) **Cu-CDA-MOF**.

**<u>Section S4</u>: A comparison of $CO_2$ uptake capacity of Cu-CDA-MOF with some recently reported MOFs.**

**Table S2.** Comparison table of $CO_2$ uptake capacity of **Cu-CDA-MOF**

| Compounds (MOFs) | $CO_2$ uptake capacity | Condition | References |
|---|---|---|---|
| **SNU-5** | 38.5 % | 273 K | *Angew. Chem., Int. Ed.* **2008**, *47*, 7741–7745. |
| **Cu-MOF** | 162.2 $cm^3$ $g^{-1}$ | 273 K | *Chem. Mater*. **2017**, *29*, 9256-9261. |
| **Cu-MOF** | 160.8 $cm^3$ $g^{-1}$ | 273 K | *J. Am. Chem. Soc*. **2016**, *138*, 2142-2145. |
| **Cu-eea-1** | 66.9 $cm^3$ $g^{-1}$ | 298 K | *Chem. Eur. J.* **2019**, *25*, 14500-14505. |
| **Cu-eea-2** | 60 $cm^3$ $g^{-1}$ | 298 K | *Chem. Eur. J.* **2019**, *25*, 14500-14505. |
| **Cu-eea-3** | 81.7 $cm^3$ $g^{-1}$ | 298 K | *Chem. Eur. J.* **2019**, *25*, 14500-14505. |
| **UTSA-74a** | 90 $cm^3$ $g^{-1}$ | 298 K | *J. Am. Chem. Soc*. **2016**, *138*, 5678-5684. |
| **Mn-act** | 43.5 $cm^3$ $g^{-1}$ | 298 K | *Chem. Eur. J.* **2016**, *22*, 7444-7451. |
| **Co-act** | 42.0 $cm^3$ $g^{-1}$ | 298 K | *Chem. Eur. J.* **2016**, *22*, 7444-7451. |
| **Ni-act** | 60.18 $cm^3$ $g^{-1}$ | 298 K | *Chem. Eur. J.* **2016**, *22*, 7444-7451. |
| **Zn-act** | 31.4 $cm^3$ $g^{-1}$ | 298 K | *Chem. Eur. J.* **2016**, *22*, 7444-7451. |
| **Cd-MOF** | 16.8 $cm^3$ $g^{-1}$ | 298 K | *J. Solid State Chem,* **2021**, *295,* 121890. |
| **Cu-CDA-MOF** | 45 $cm^3$ $g^{-1}$ | 298 K | **This work** |

## Section S5: Knoevenagel Condensation Reaction Catalyzed by Cd-CDA-MOF

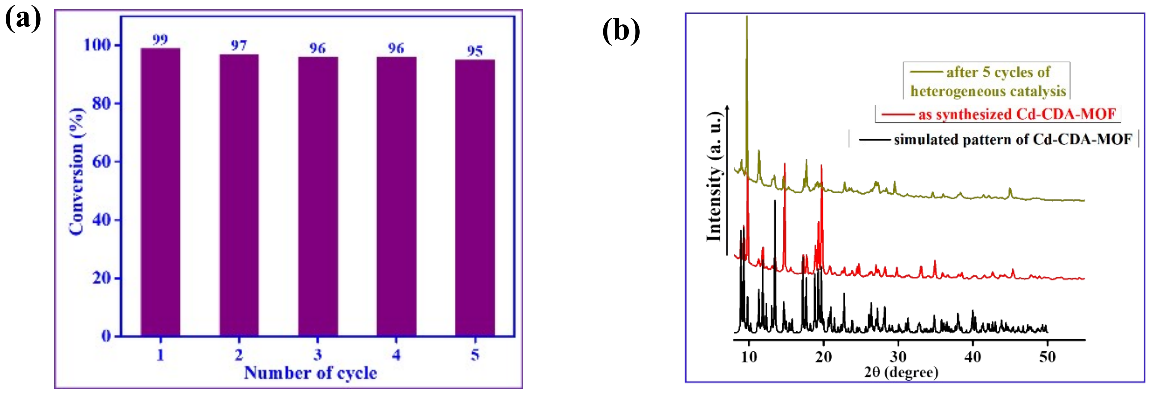


**Figure S3.** (a) Recyclability experiment of **Cd-CDA-MOF** catalyst for Knoevenagel condensation reaction; (b) comparison of PXRD pattern after successive five cycles of reactions.

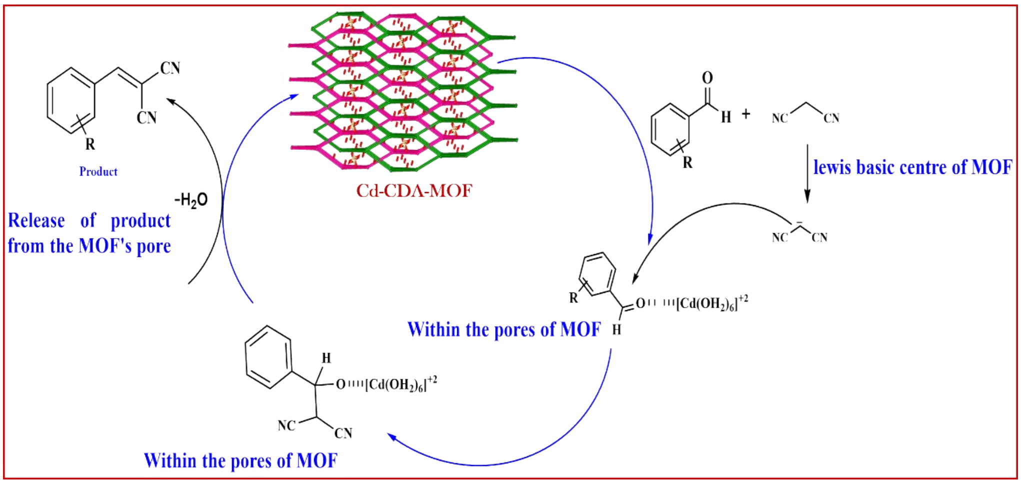


**Scheme S1.** A schematic for plausible mechanism of Knoevenagel condensation reaction catalyzed by **Cd-CDA-MOF**.

## Section S6: Chan-Lam Coupling Reaction Catalyzed by Cu-CDA-MOF

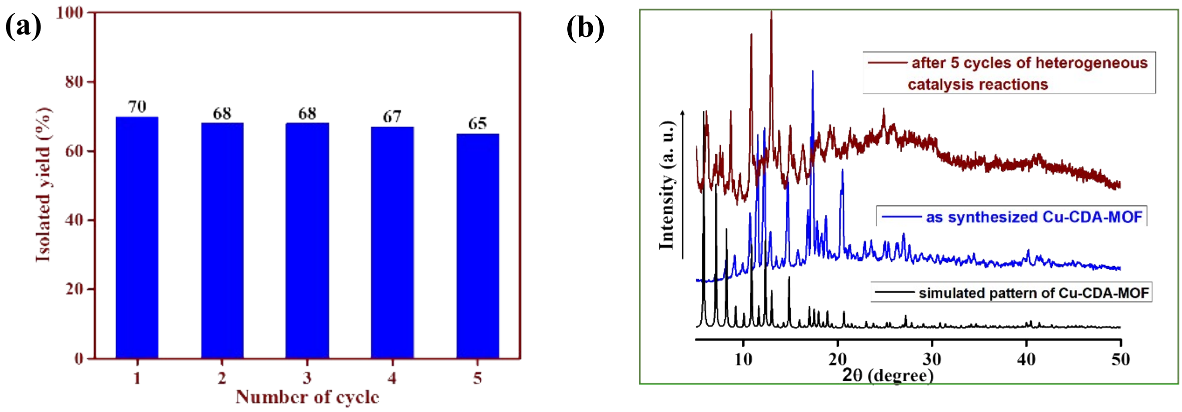


**Figure S4.** (a) Recyclability experiment of **Cu-CDA-MOF** catalyst for Chan-Lam coupling reaction; (b) comparison of PXRD pattern after successive five cycles of reactions.

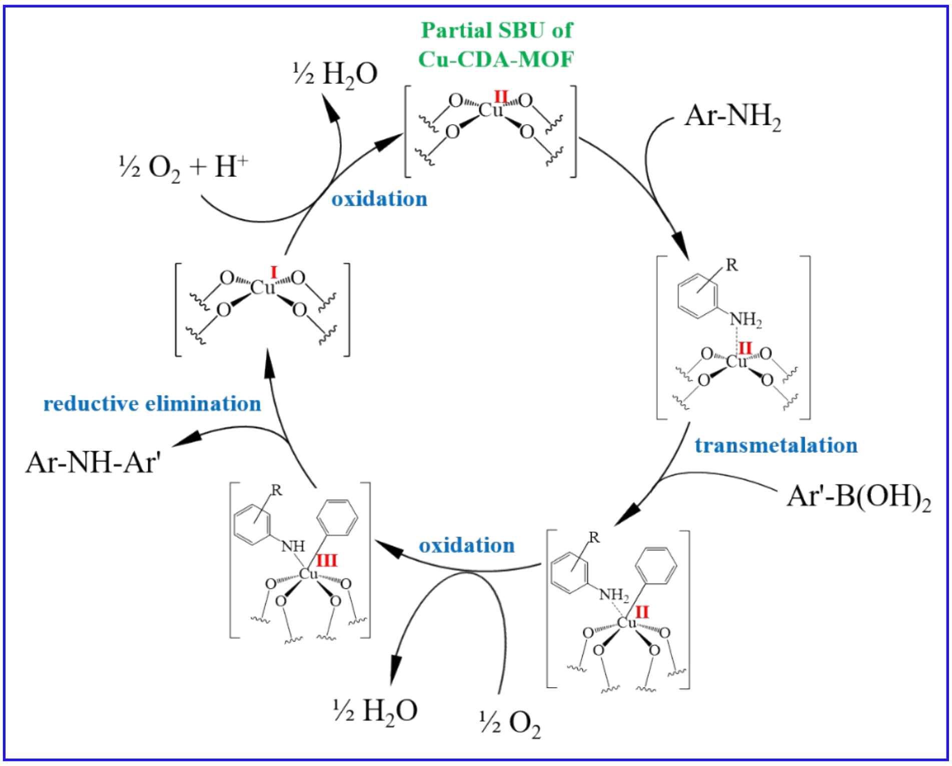


**Scheme S2.** A schematic for plausible mechanism of Chan-Lam coupling reaction catalyzed by **Cu-CDA-MOF**.

**<u>Section S7</u>: Representative $^{1}H$ and $^{13}C$ NMR Spectra**

**<u>Section S7a</u>: Representative $^{1}H$ and $^{13}C$ NMR Spectra of Knoevenagel Condensation Products**

(a)

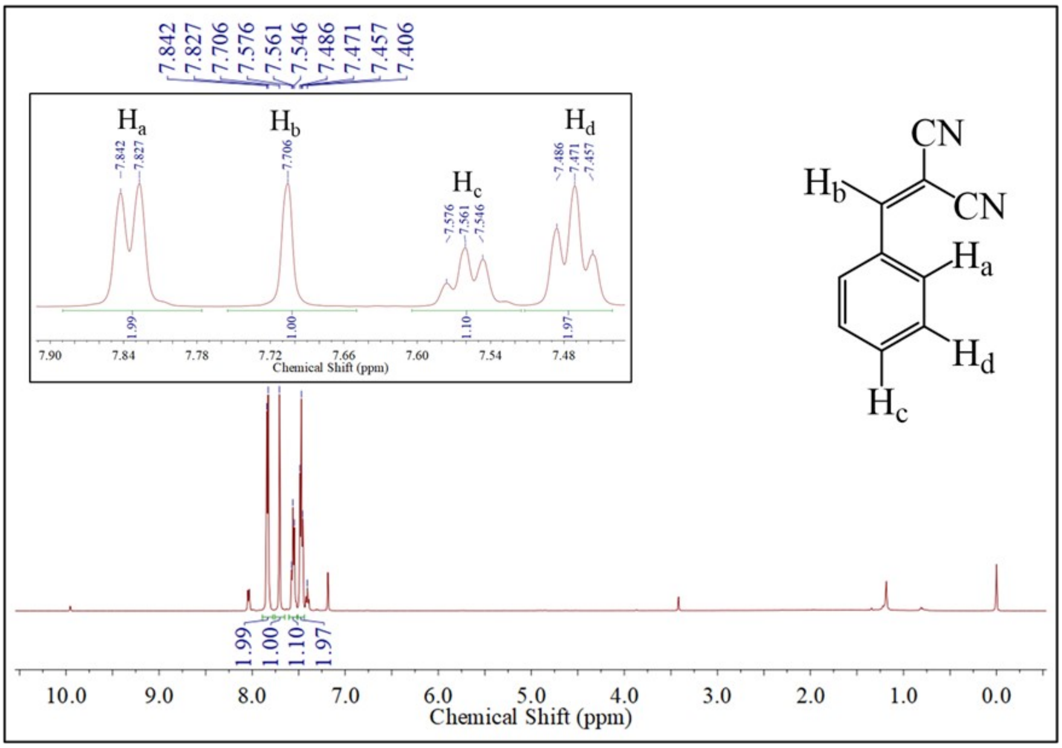


(b)

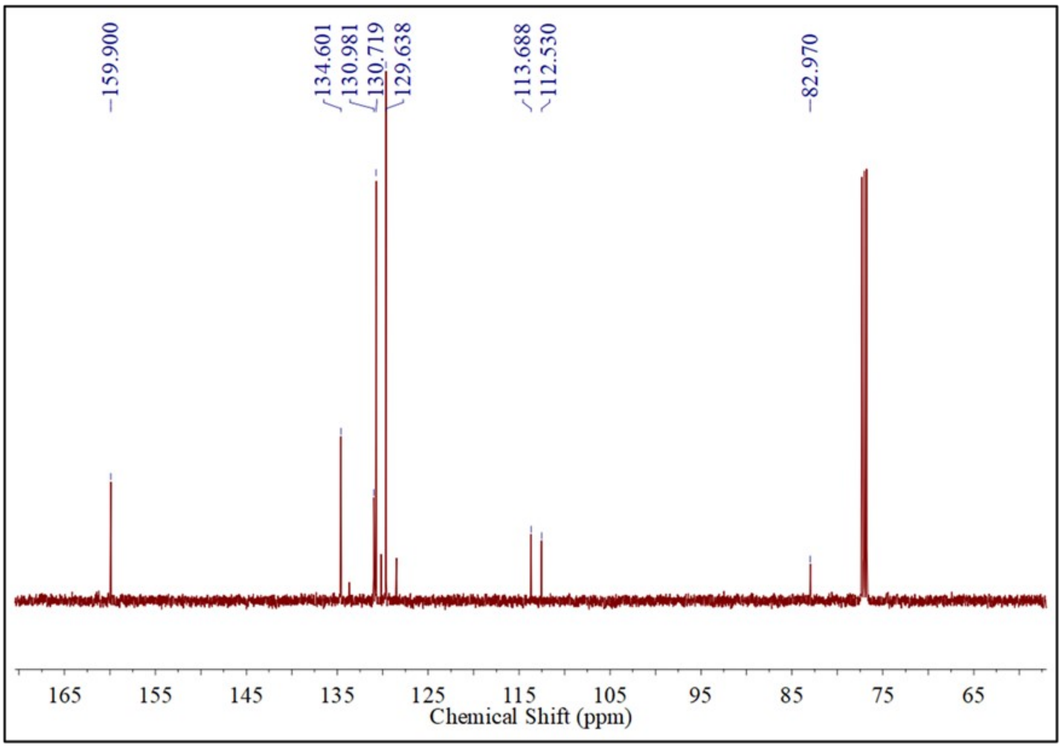


**Figure S5.** (a) $^{1}H$ NMR ($CDCl_3$, 500 MHz) and (b) $^{13}C$ ($CDCl_3$, 500 MHz) of Knoevenagel Condensation product of benzaldehyde and malononitrile catalyzed by **Cd-CDA-MOF**

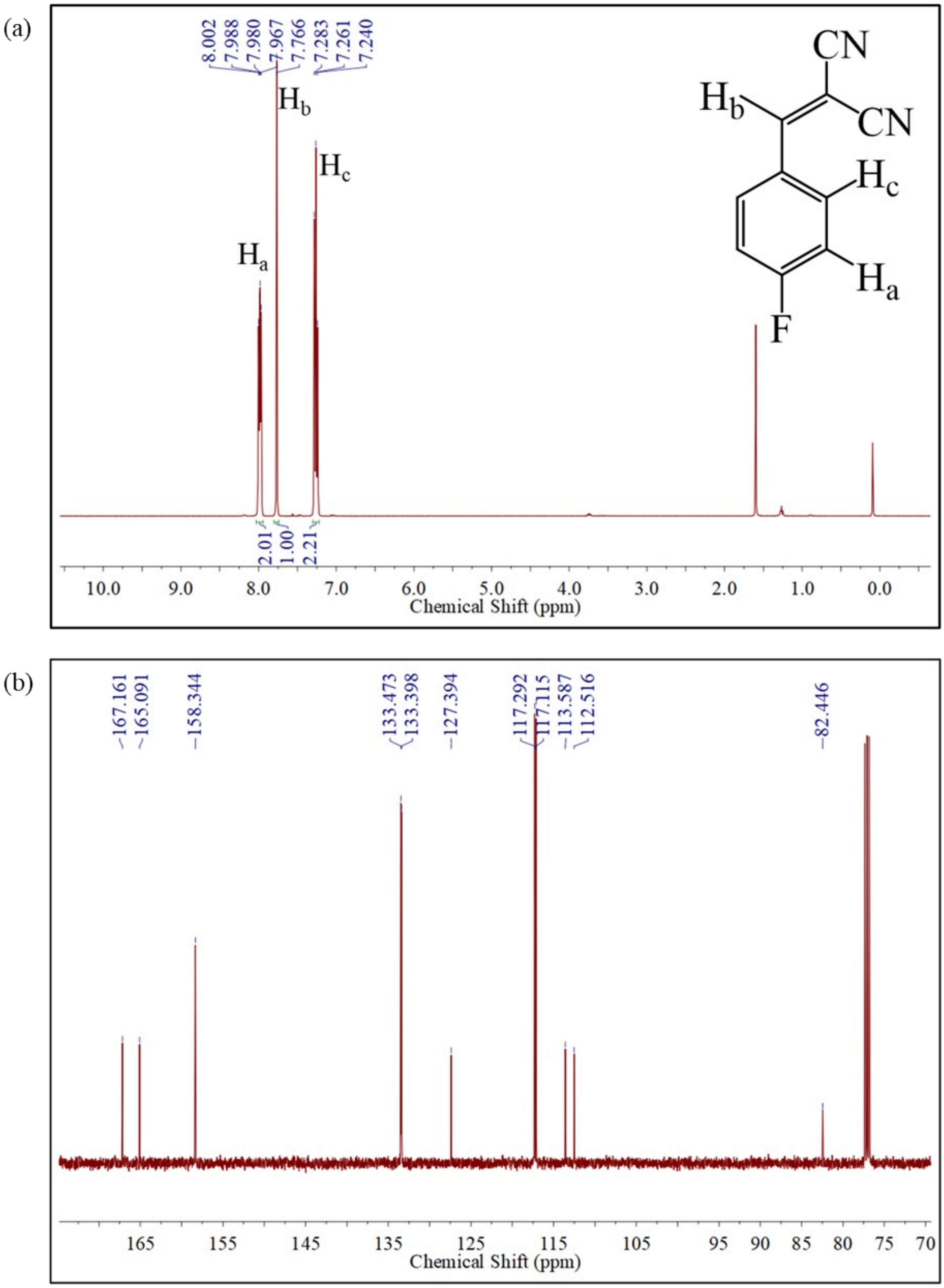


**Figure S6.** (a) $^{1}H$ NMR ($CDCl_3$, 400 MHz) and (b) $^{13}C$ ($CDCl_3$, 500 MHz) of Knoevenagel Condensation product of 4-fluorobenzaldehyde and malononitrile catalyzed by **Cd-CDA-MOF**.

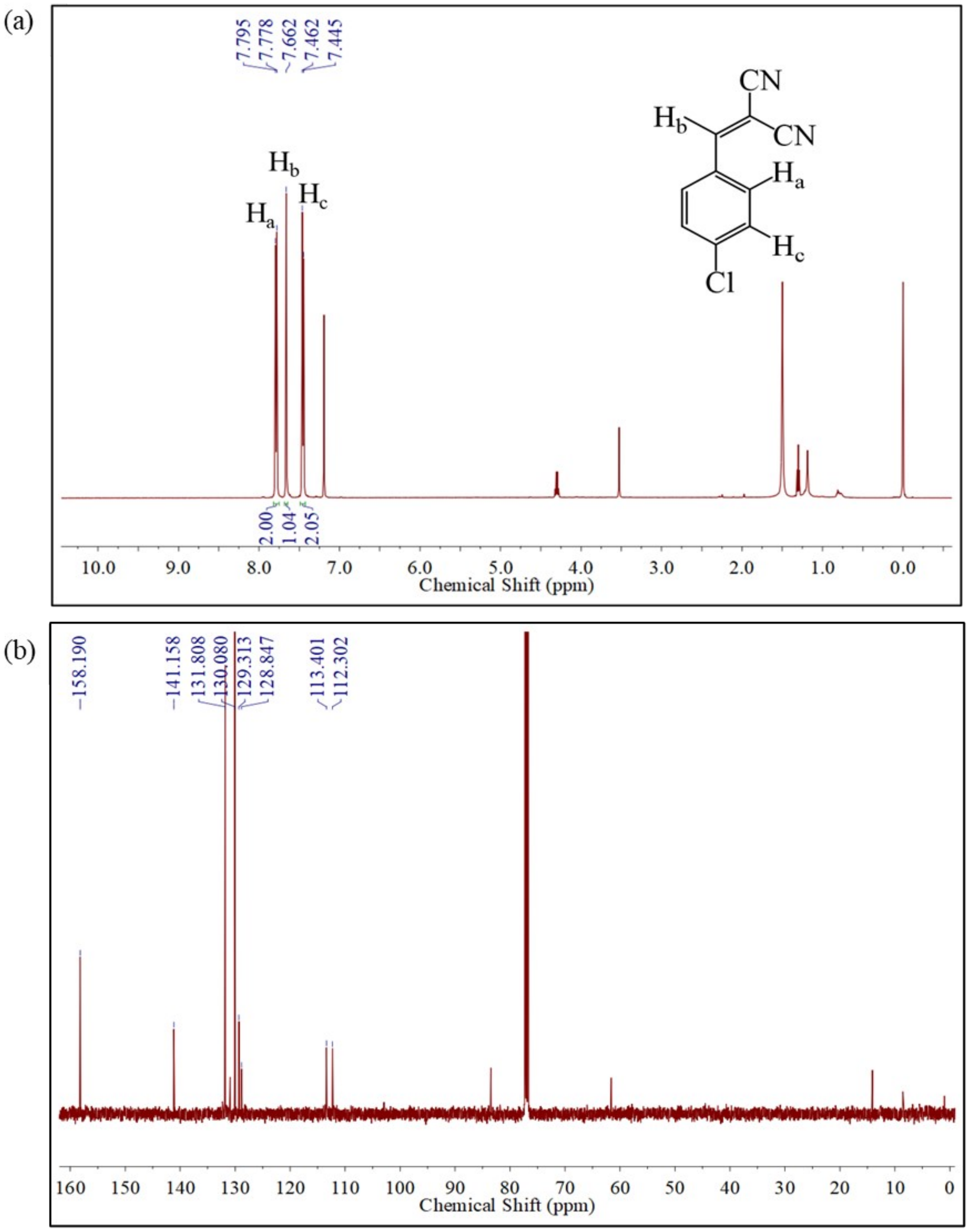


**Figure S7.** (a) $^{1}$H NMR ($CDCl_3$, 500 MHz) and (b) $^{13}$C ($CDCl_3$, 500 MHz) of Knoevenagel Condensation product of 4-chlorobenzaldehyde and malononitrile catalyzed by **Cd-CDA-MOF.**

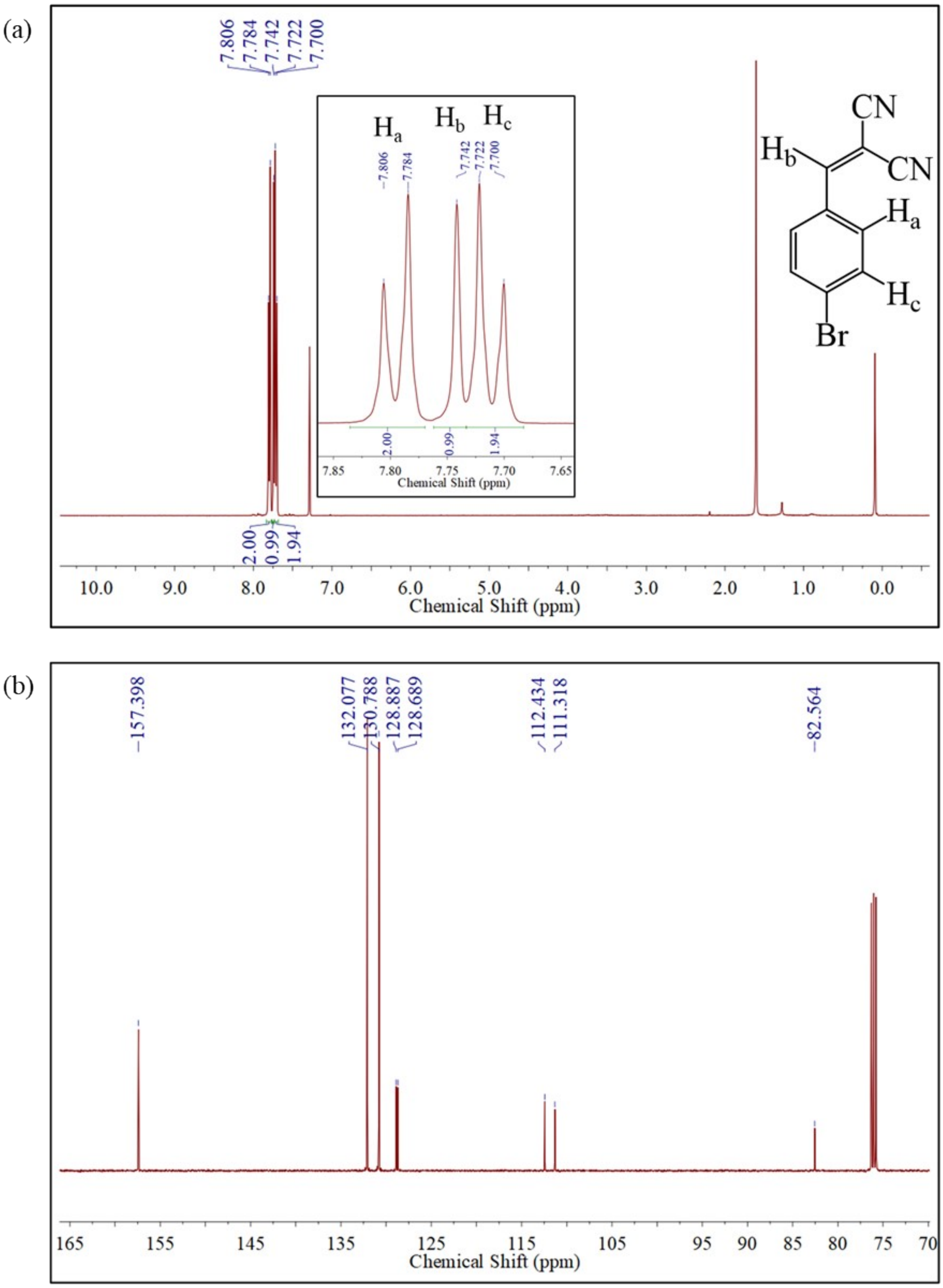


**Figure S8.** (a) $^1$H NMR ($CDCl_3$, 400 MHz) and (b) $^{13}$C ($CDCl_3$, 500 MHz) of Knoevenagel Condensation product of 4-bromobenzaldehyde and malononitrile catalyzed by **Cd-CDA-MOF**.

(a)

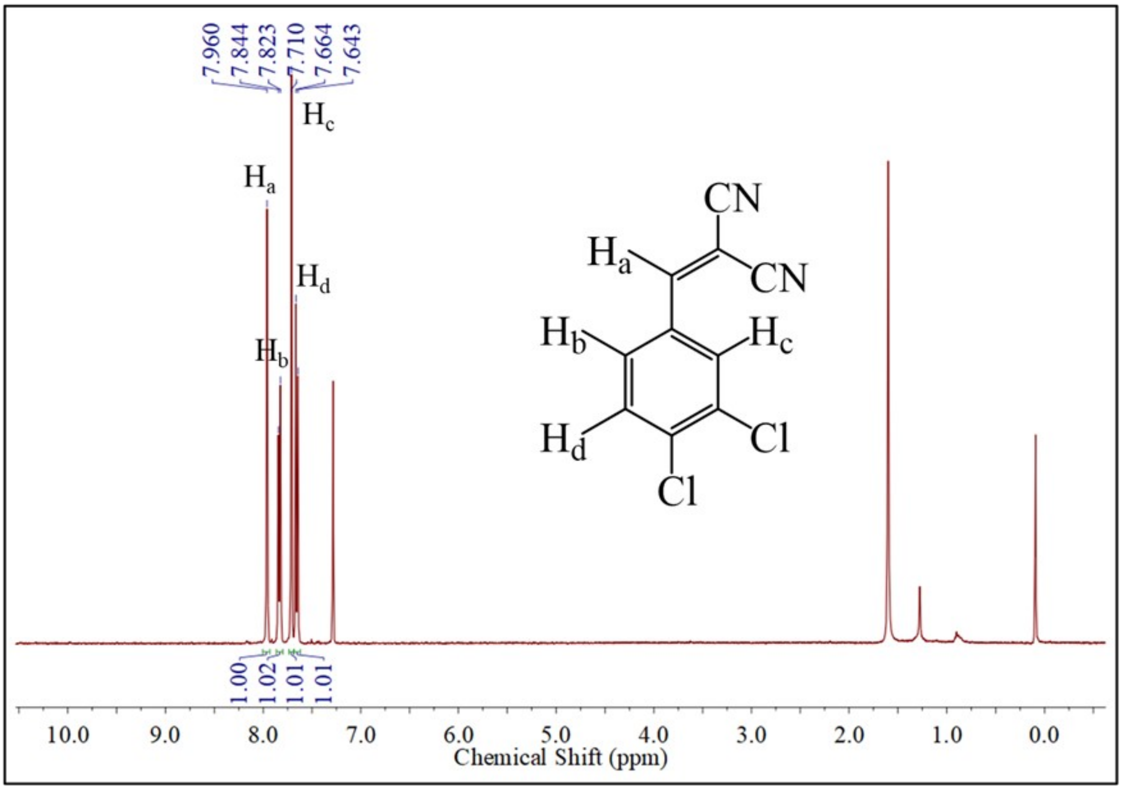


(b)

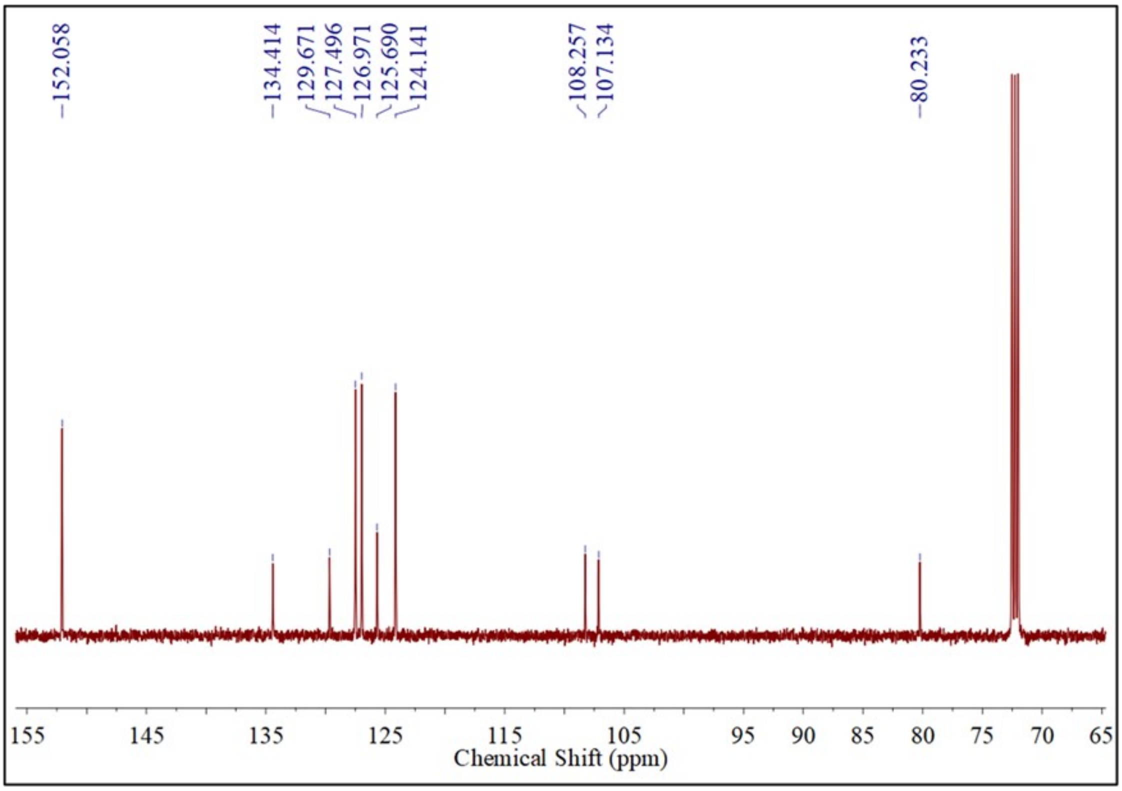


**Figure S9.** (a) $^{1}H$ NMR ($CDCl_3$, 400 MHz) and (b) $^{13}C$ ($CDCl_3$, 500 MHz) of Knoevenagel Condensation product of 3,4-dichlorobenzaldehyde and malononitrile catalyzed by **Cd-CDA-MOF**.

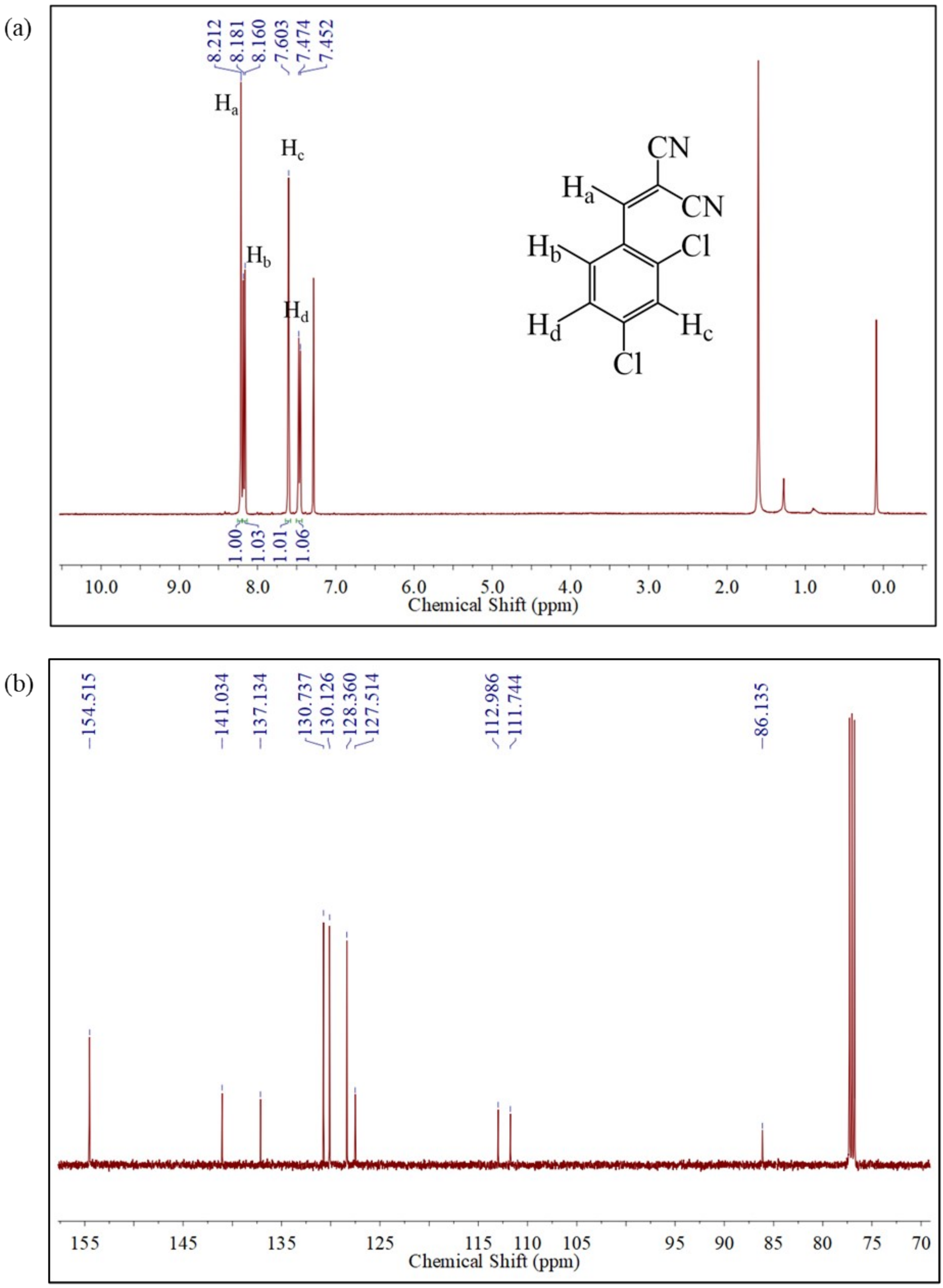


**Figure S10.** (a) $^{1}$H NMR ($CDCl_3$, 400 MHz) and (b) $^{13}$C ($CDCl_3$, 500 MHz) of Knoevenagel Condensation product of 2,4-dichlorobenzaldehyde and malononitrile catalyzed by **Cd-CDA-MOF**.

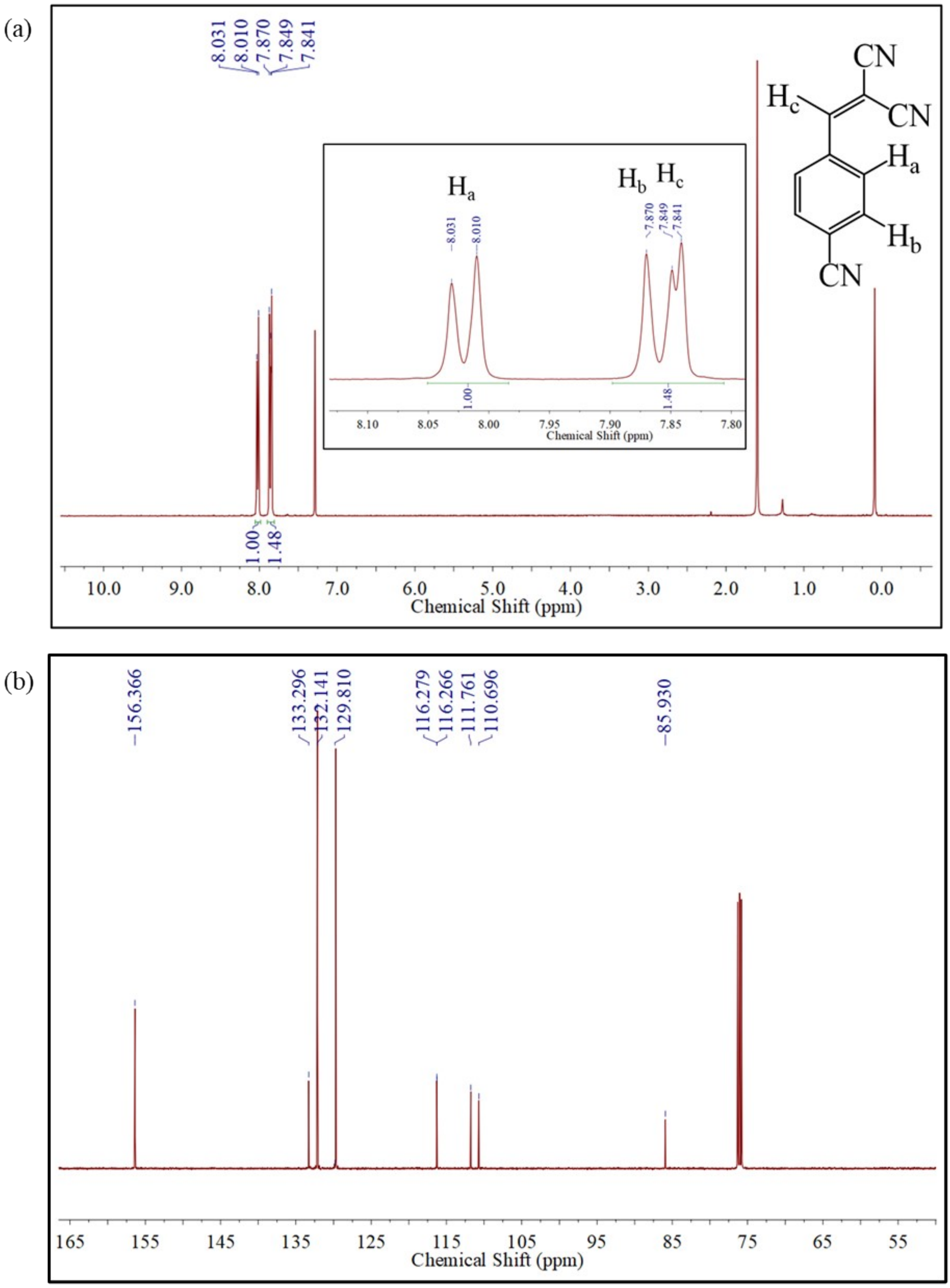


**Figure S11.** (a) $^1H$ NMR ($CDCl_3$, 400 MHz) and (b) $^{13}C$ ($CDCl_3$, 500 MHz) of Knoevenagel Condensation product of 4-cyanobenzaldehyde and malononitrile catalyzed by **Cd-CDA-MOF**.

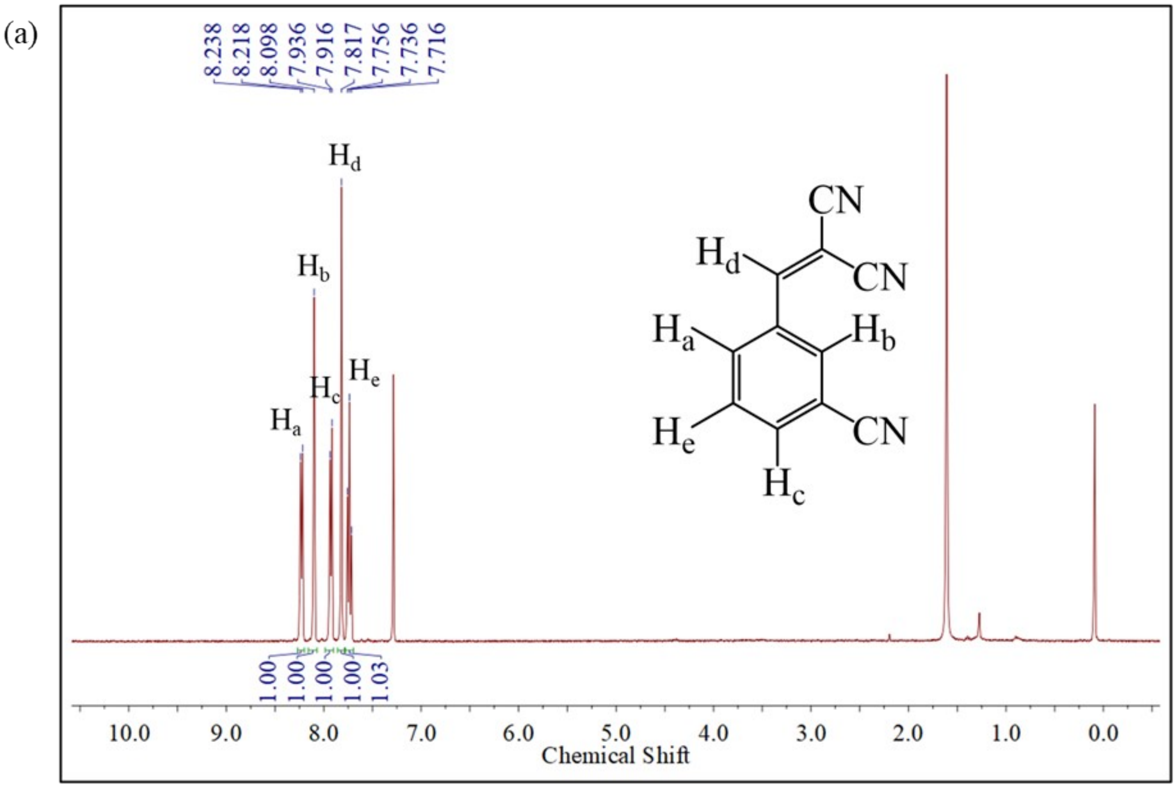


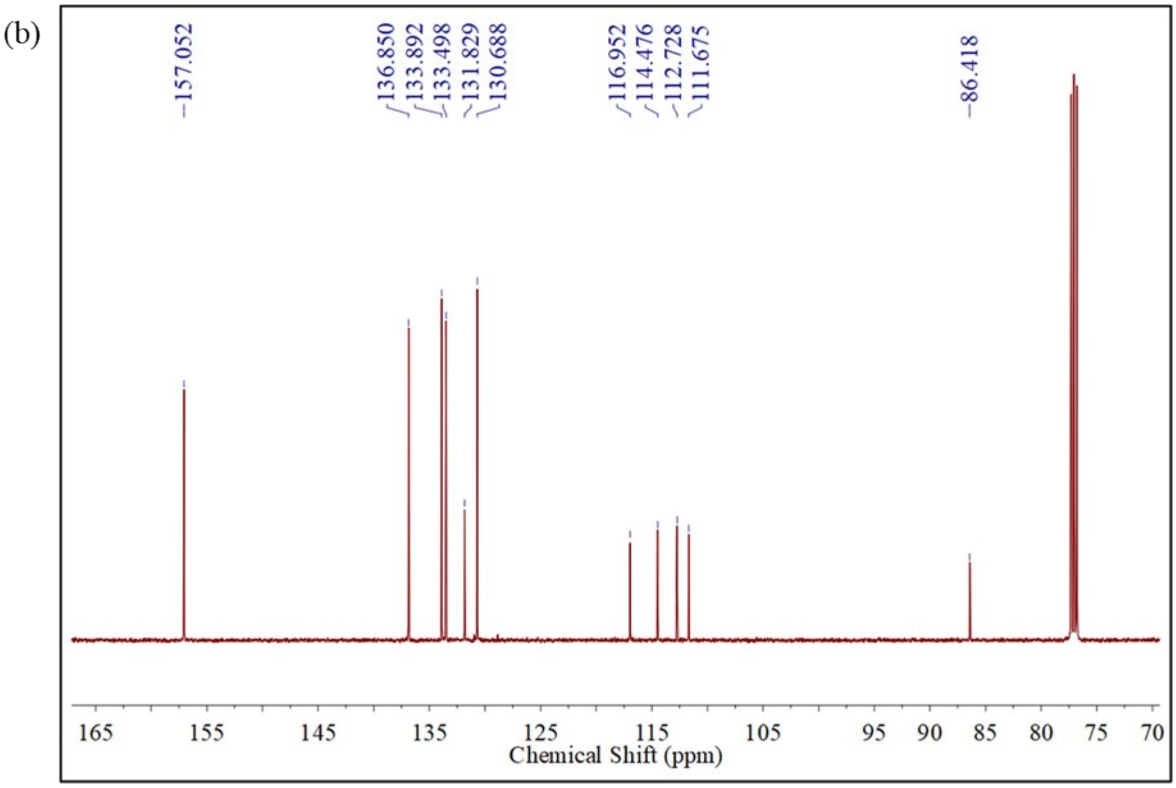


**Figure S12.** (a) $^{1}H$ NMR ($CDCl_3$, 400 MHz) and (b) $^{13}C$ ($CDCl_3$, 500 MHz) of Knoevenagel Condensation product of 3-cyanobenzaldehyde and malononitrile catalyzed by **Cd-CDA-MOF.**

(a)

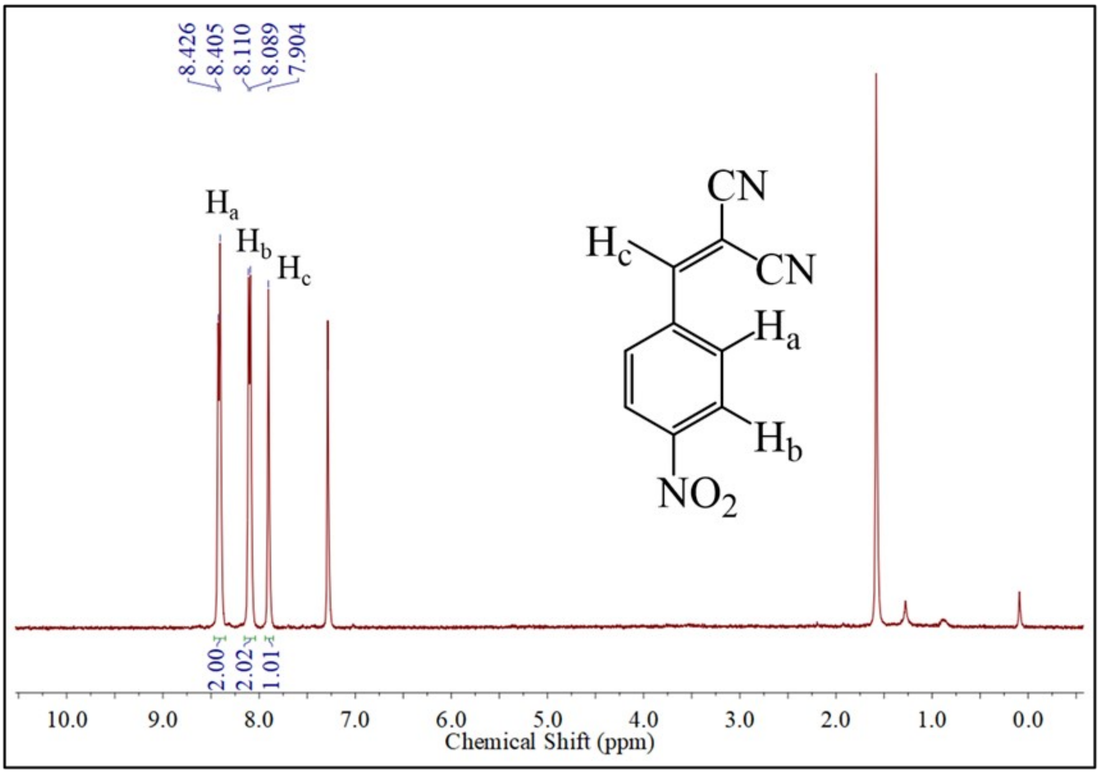


(b)

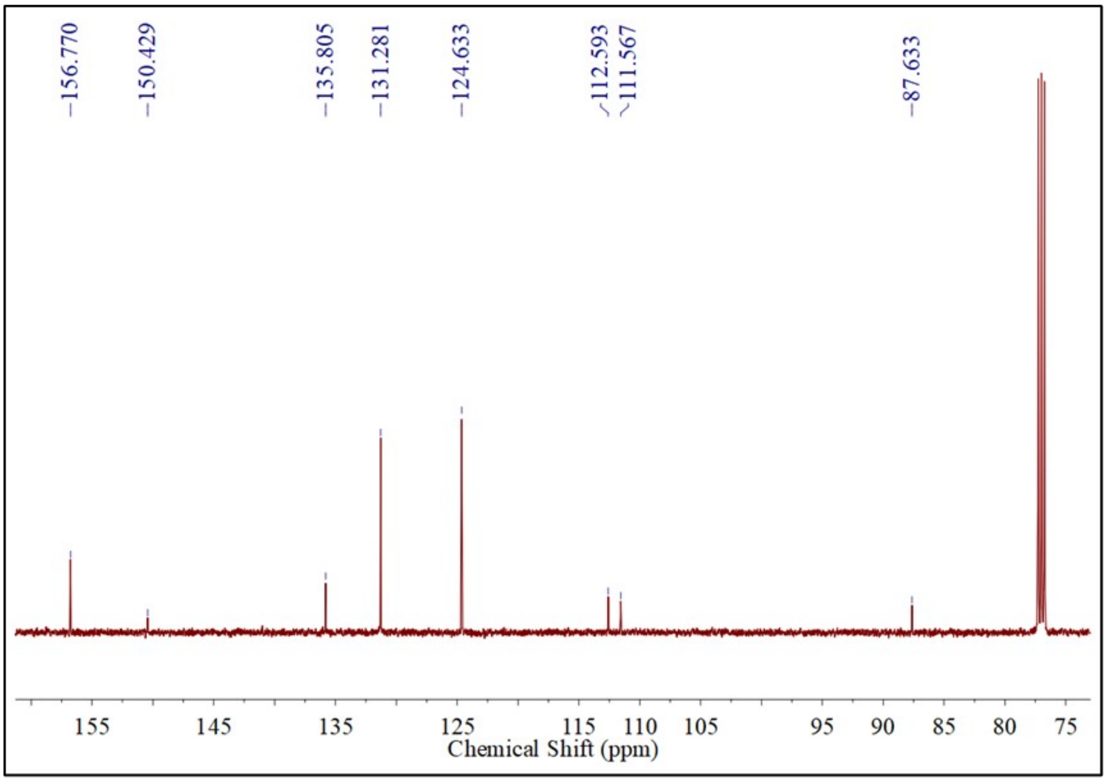


**Figure S13.** (a) $^1$H NMR ($CDCl_3$, 400 MHz) and (b) $^{13}$C ($CDCl_3$, 500 MHz) of Knoevenagel Condensation product of 4-nitrobenzaldehyde and malononitrile catalyzed by **Cd-CDA-MOF**.

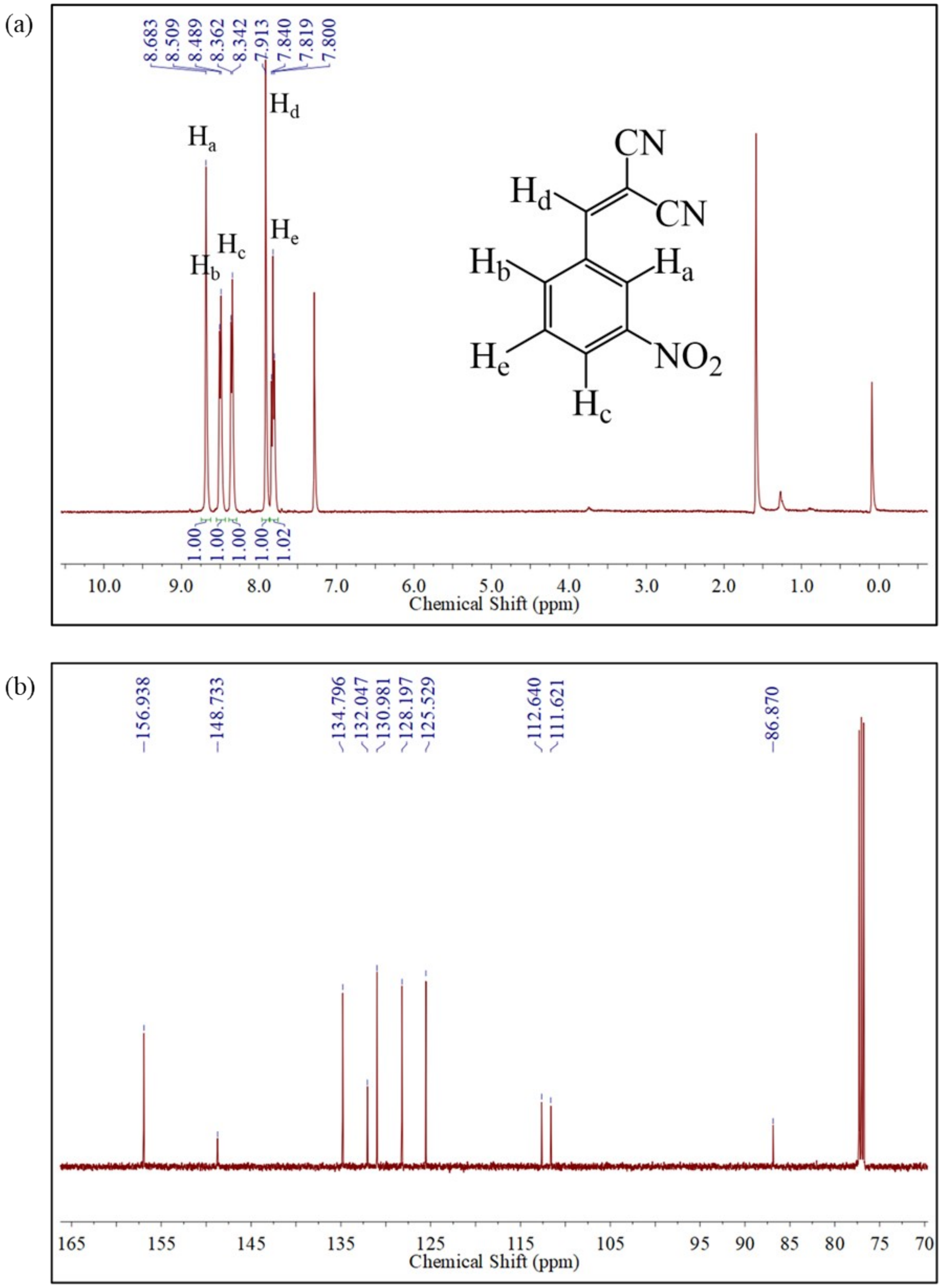


**Figure S14.** (a) $^1$H NMR ($CDCl_3$, 400 MHz) and (b) $^{13}$C ($CDCl_3$, 500 MHz) of Knoevenagel Condensation product of 3-nitrobenzaldehyde and malononitrile catalyzed by **Cd-CDA-MOF**.

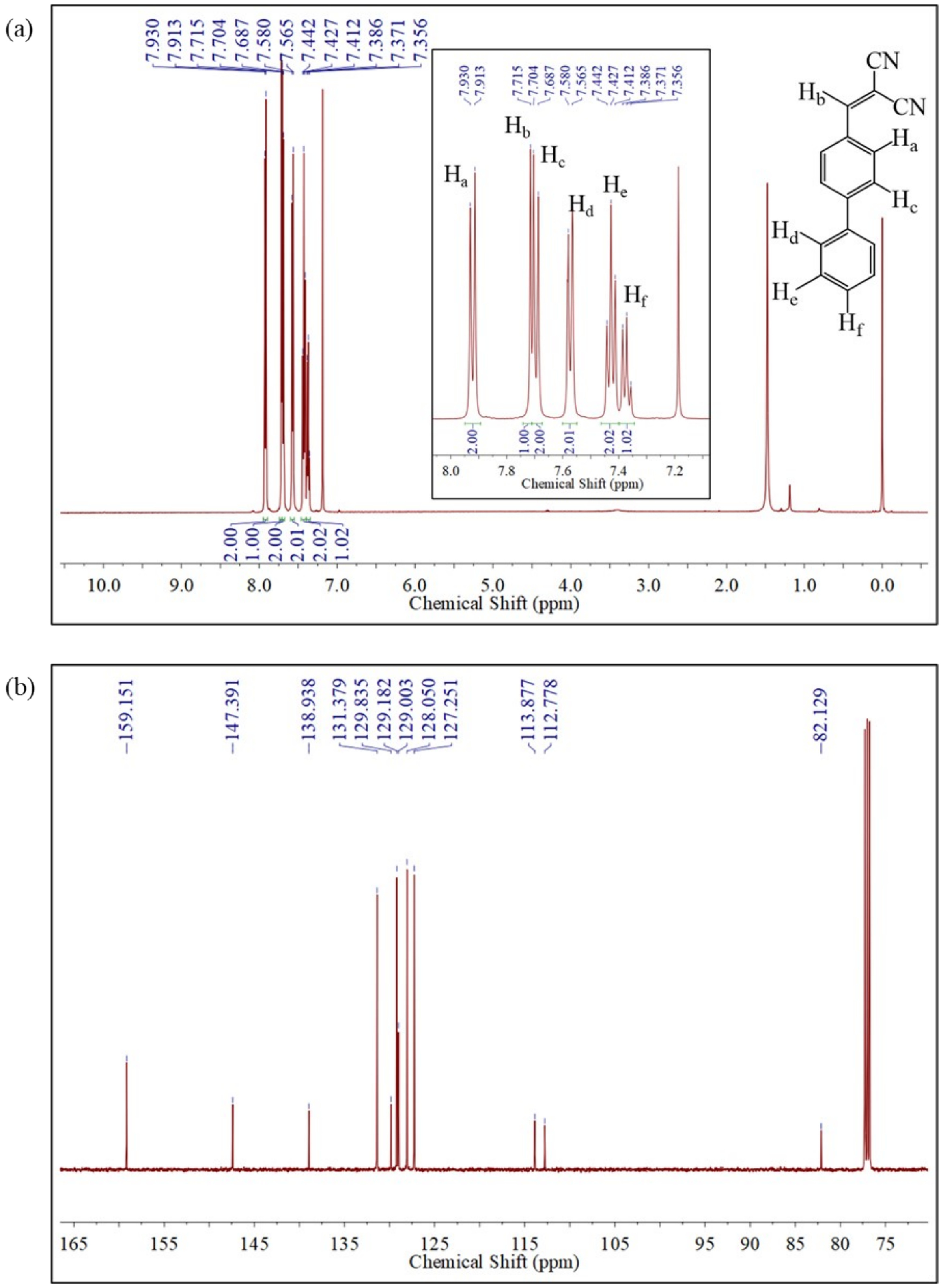


**Figure S15.** (a) $^{1}H$ NMR ($CDCl_3$, 500 MHz) and (b) $^{13}C$ ($CDCl_3$, 500 MHz) of Knoevenagel Condensation product of 4-phenylbenzaldehyde and malononitrile catalyzed by **Cd-CDA-MOF**.

(a)

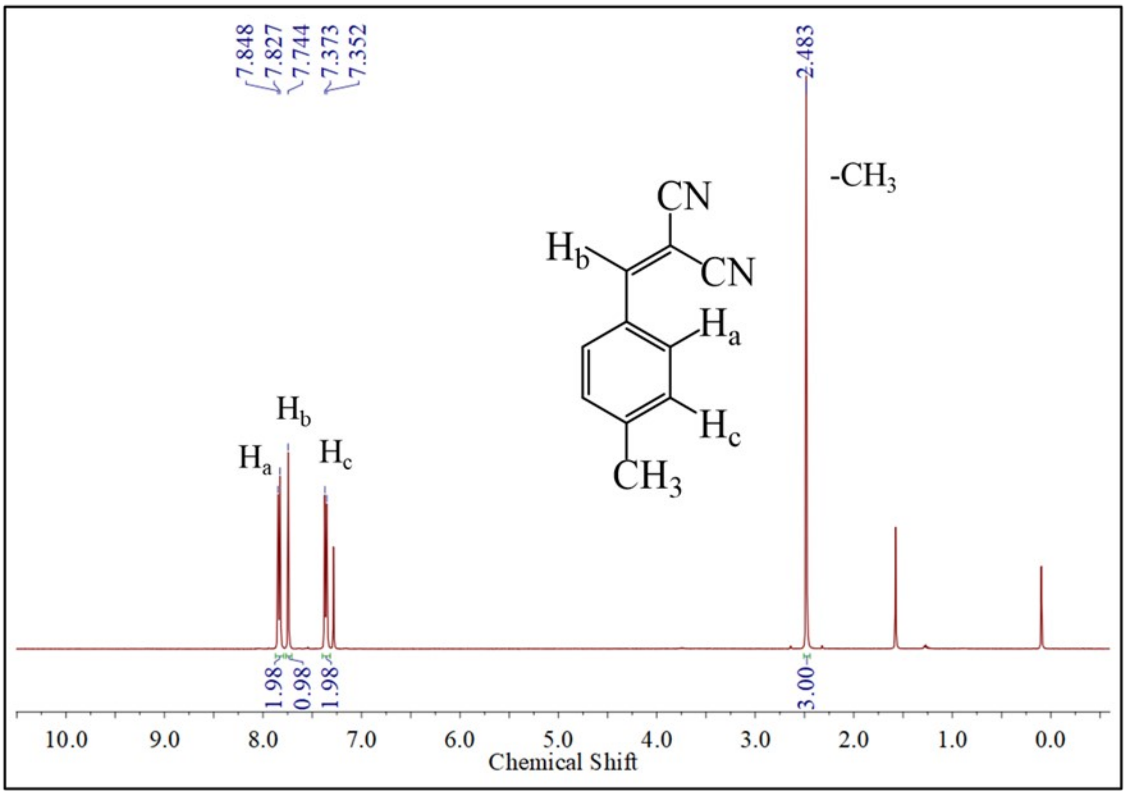


(b)

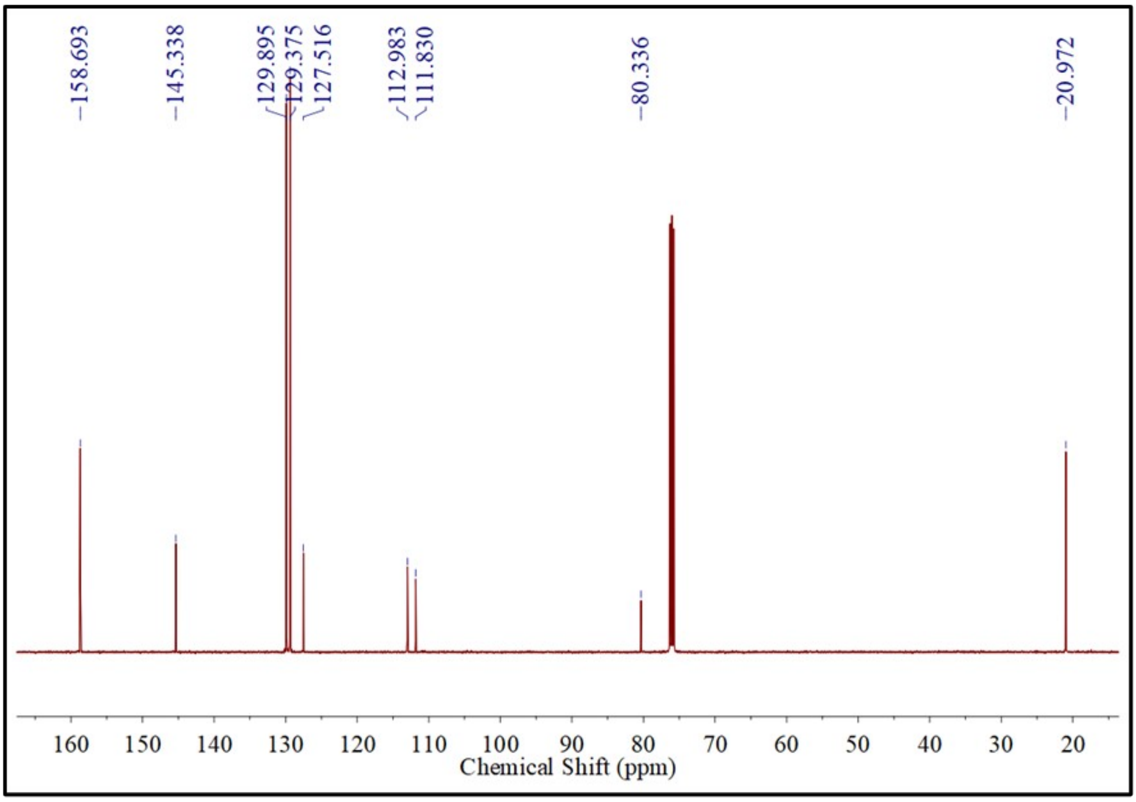


**Figure S16.** (a) $^{1}H$ NMR ($CDCl_3$, 400 MHz) and (b) $^{13}C$ ($CDCl_3$, 500 MHz) of Knoevenagel Condensation product of 4-methylbenzaldehyde and malononitrile catalyzed by **Cd-CDA-MOF**.

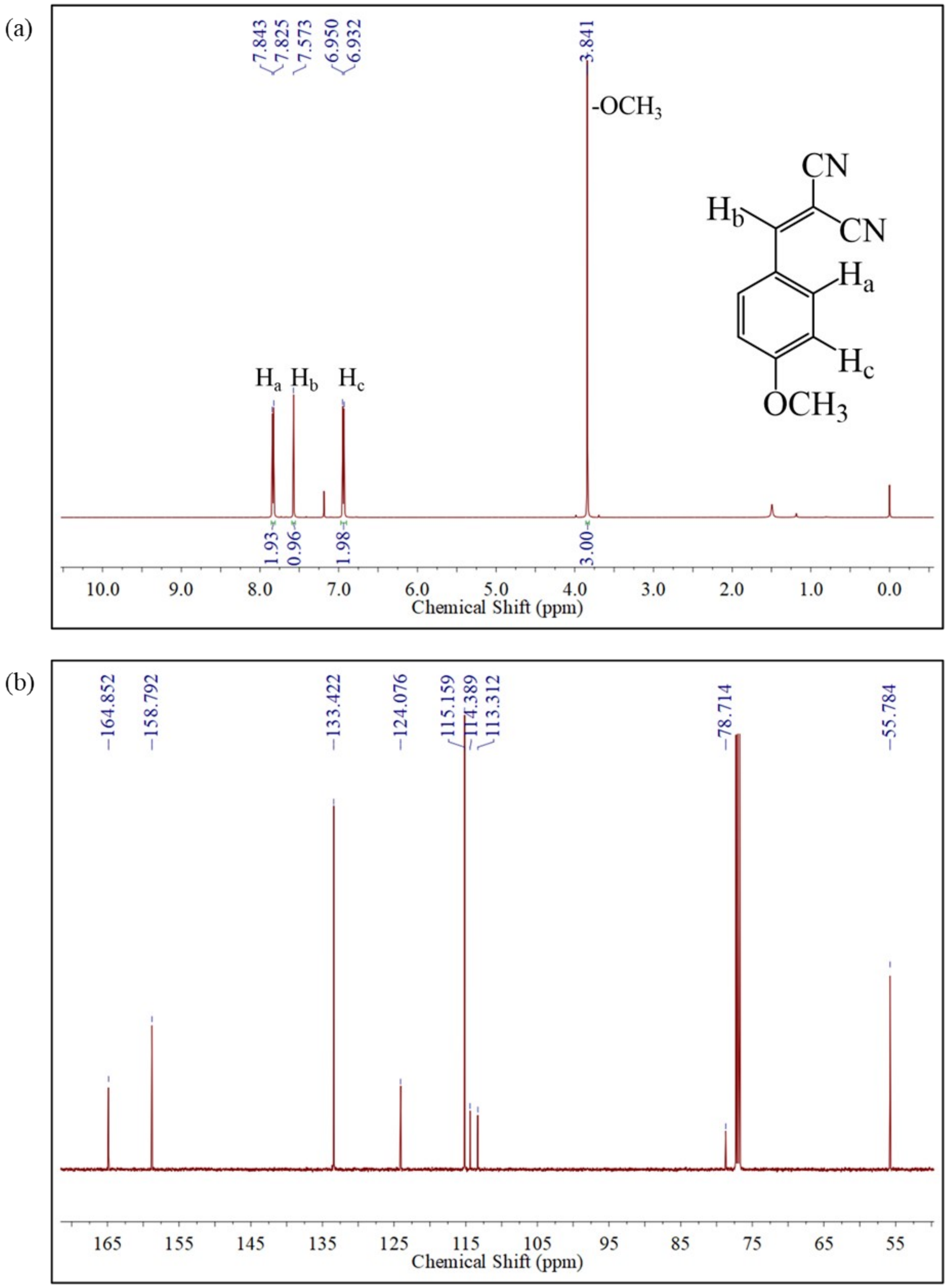


**Figure S17.** (a) [1]H NMR ($CDCl_3$, 500 MHz) and (b) [13]C ($CDCl_3$, 500 MHz) of Knoevenagel Condensation product of 4-methoxybenzaldehyde and malononitrile catalyzed by **Cd-CDA-MOF**

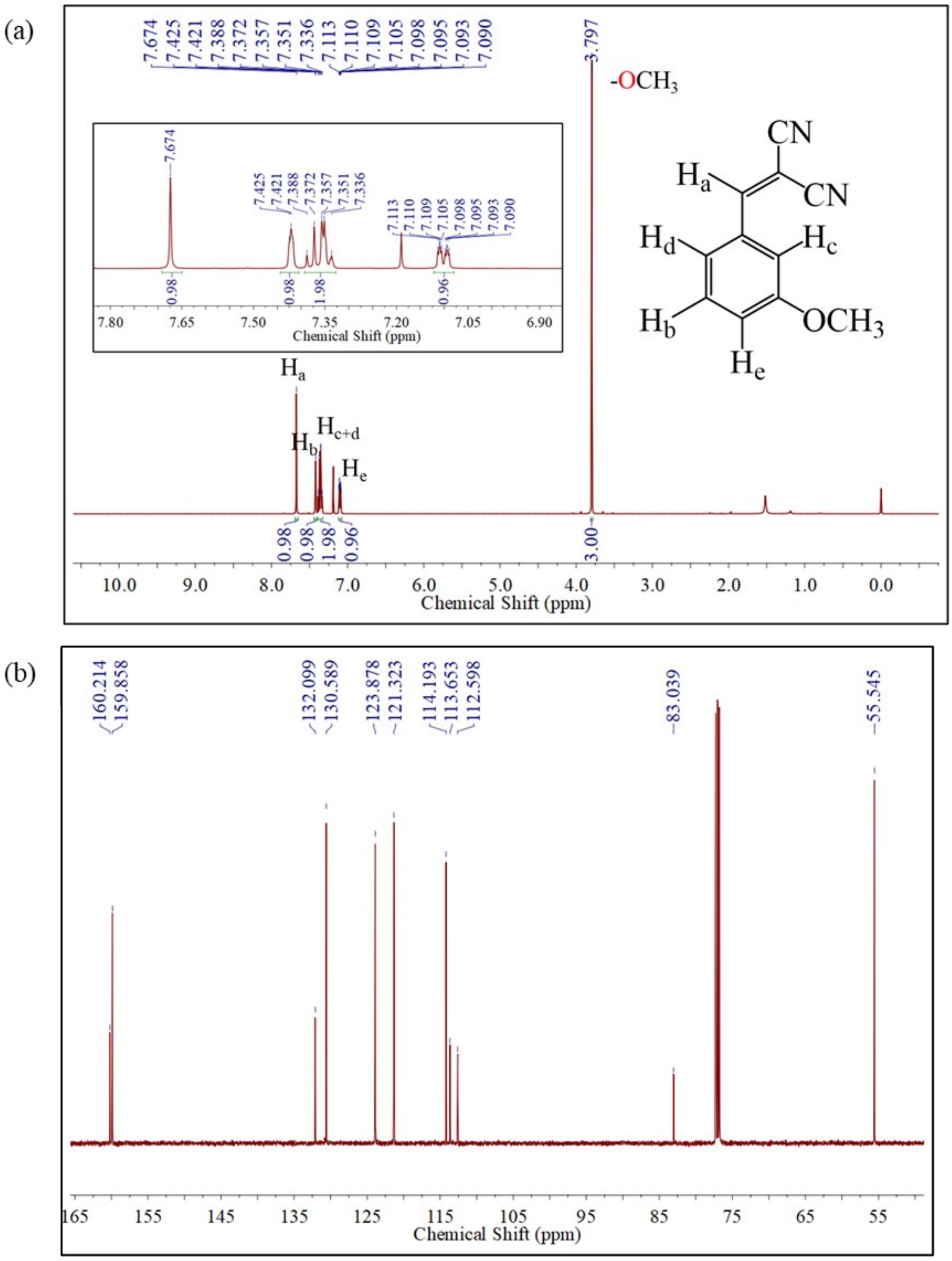


**Figure S18.** (a) $^{1}H$ NMR ($CDCl_3$, 500 MHz) and (b) $^{13}C$ ($CDCl_3$, 500 MHz) of Knoevenagel Condensation product of 3-methoxybenzaldehyde and malononitrile catalyzed by **Cd-CDA-MOF**.

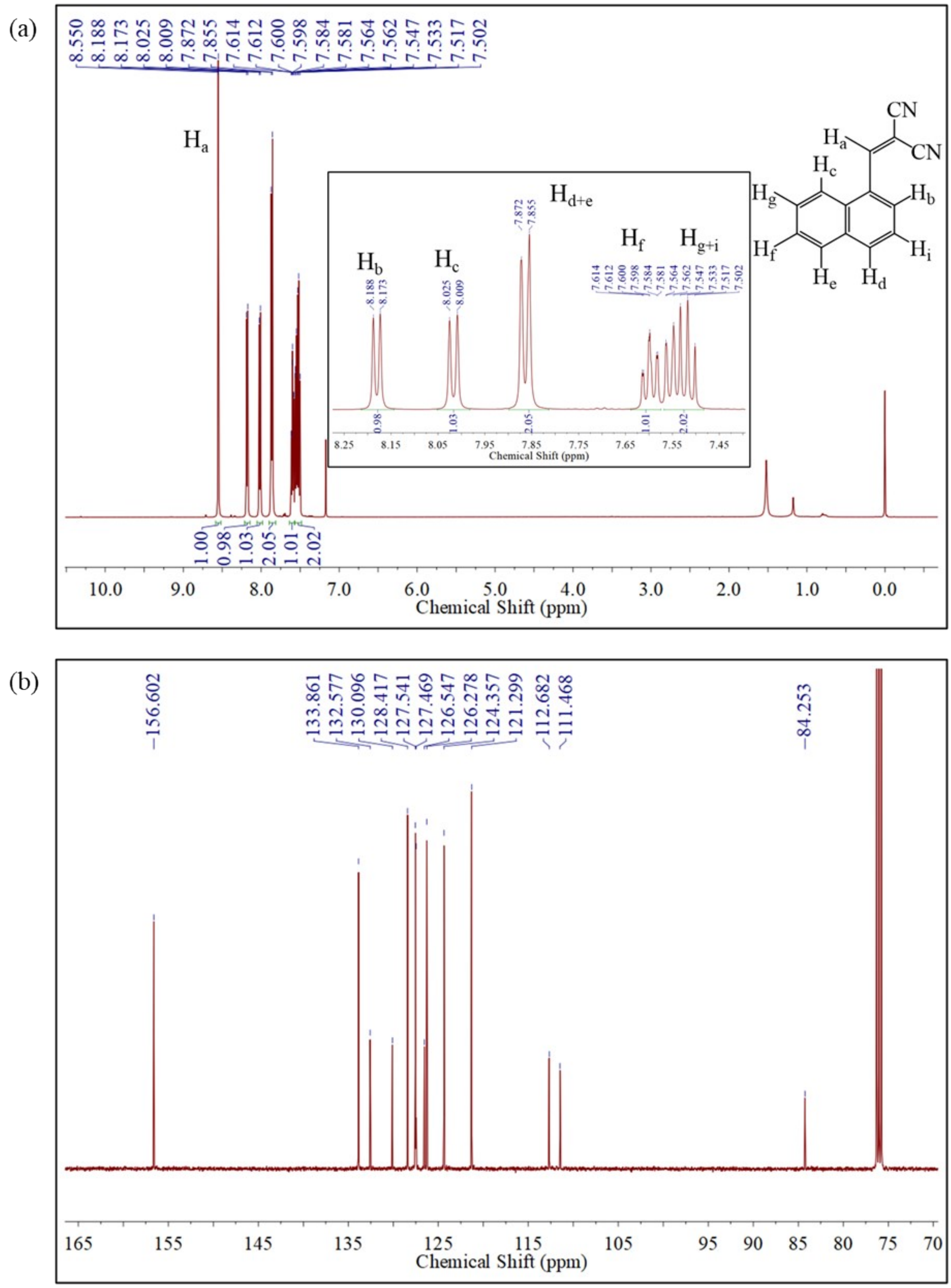


**Figure S19.** (a) $^{1}$H NMR ($CDCl_3$, 500 MHz) and (b) $^{13}$C ($CDCl_3$, 500 MHz) of Knoevenagel Condensation product of 1-napthaldehyde and malononitrile catalyzed by **Cd-CDA-MOF**.

**<u>Section S7b</u>: Representative $^{1}H$ and $^{13}C$ NMR Spectra of Chan-Lam Coupling Products**

(a)

(b)

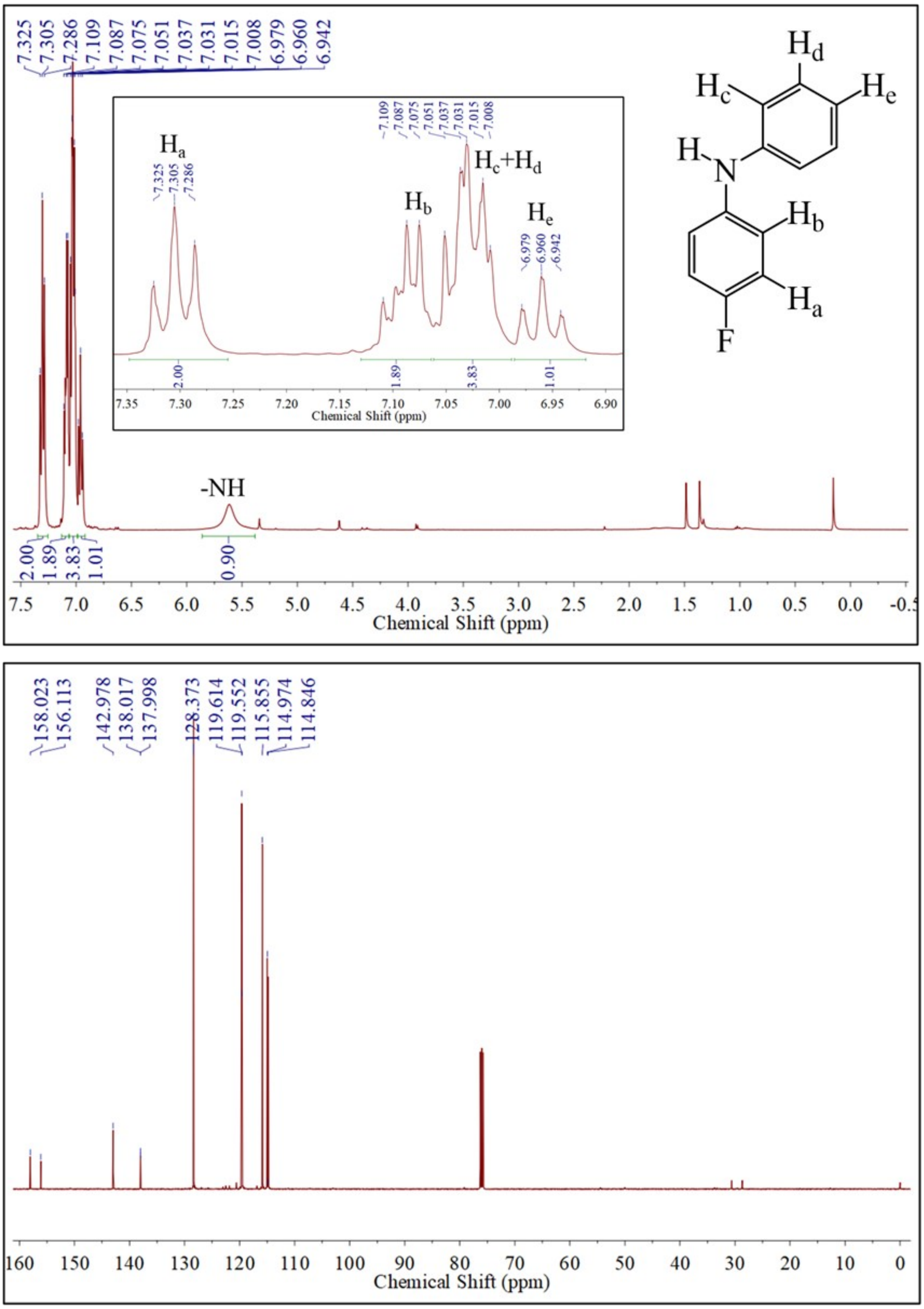


**Figure S20.** (a) $^{1}H$ NMR ($CDCl_3$, 400 MHz) and (b) $^{13}C$ ($CDCl_3$, 500 MHz) of Chan-Lam coupling product of 4-fluoroaniline and phenylboronic acid catalyzed by **Cu-CDA-MOF**.

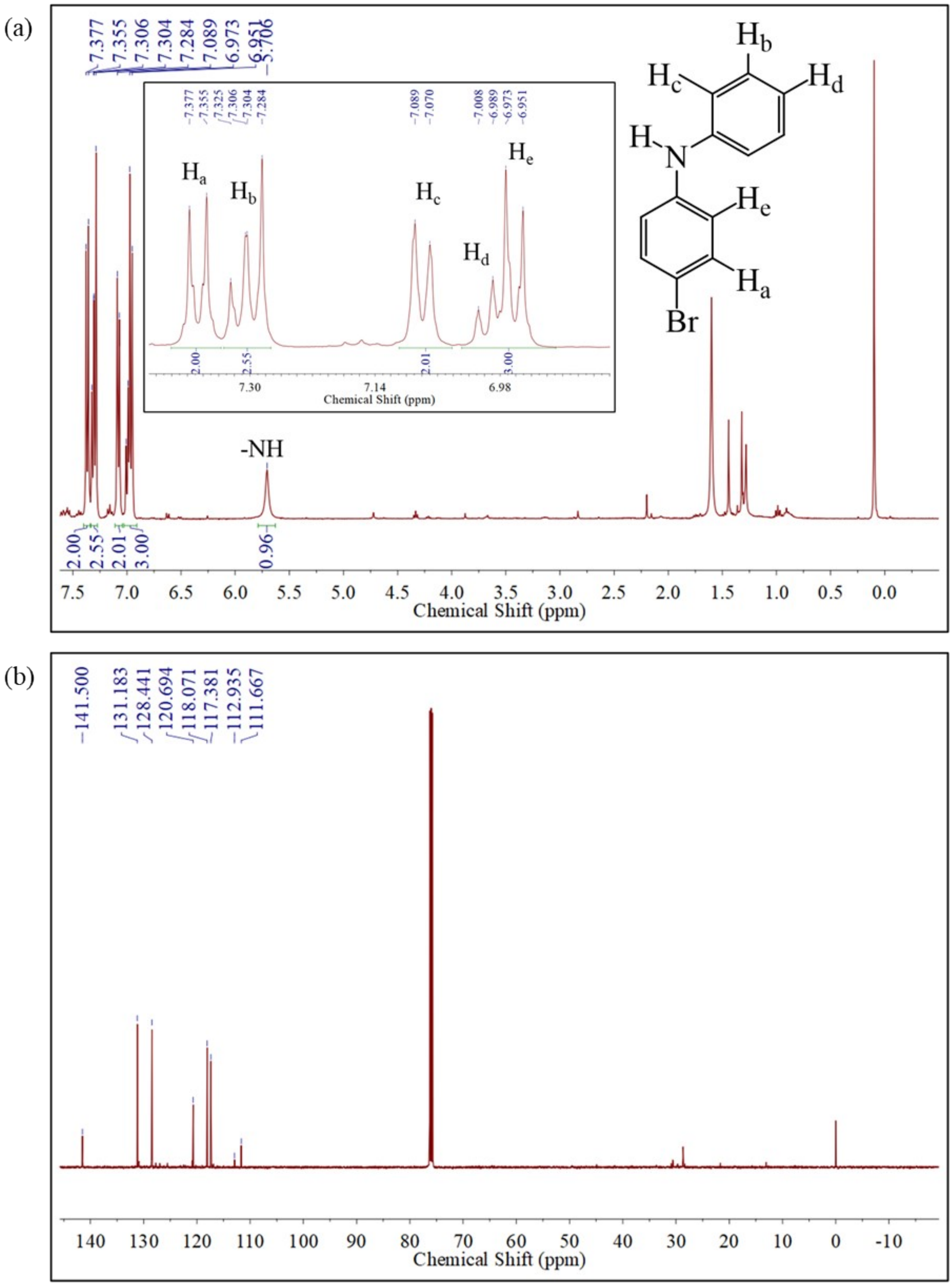


**Figure S21.** (a) $^{1}H$ NMR ($CDCl_3$, 400 MHz) and (b) $^{13}C$ ($CDCl_3$, 500 MHz) of Chan-Lam coupling product of 4-bromoaniline and phenylboronic acid catalyzed by **Cu-CDA-MOF.**

(a)

(b)

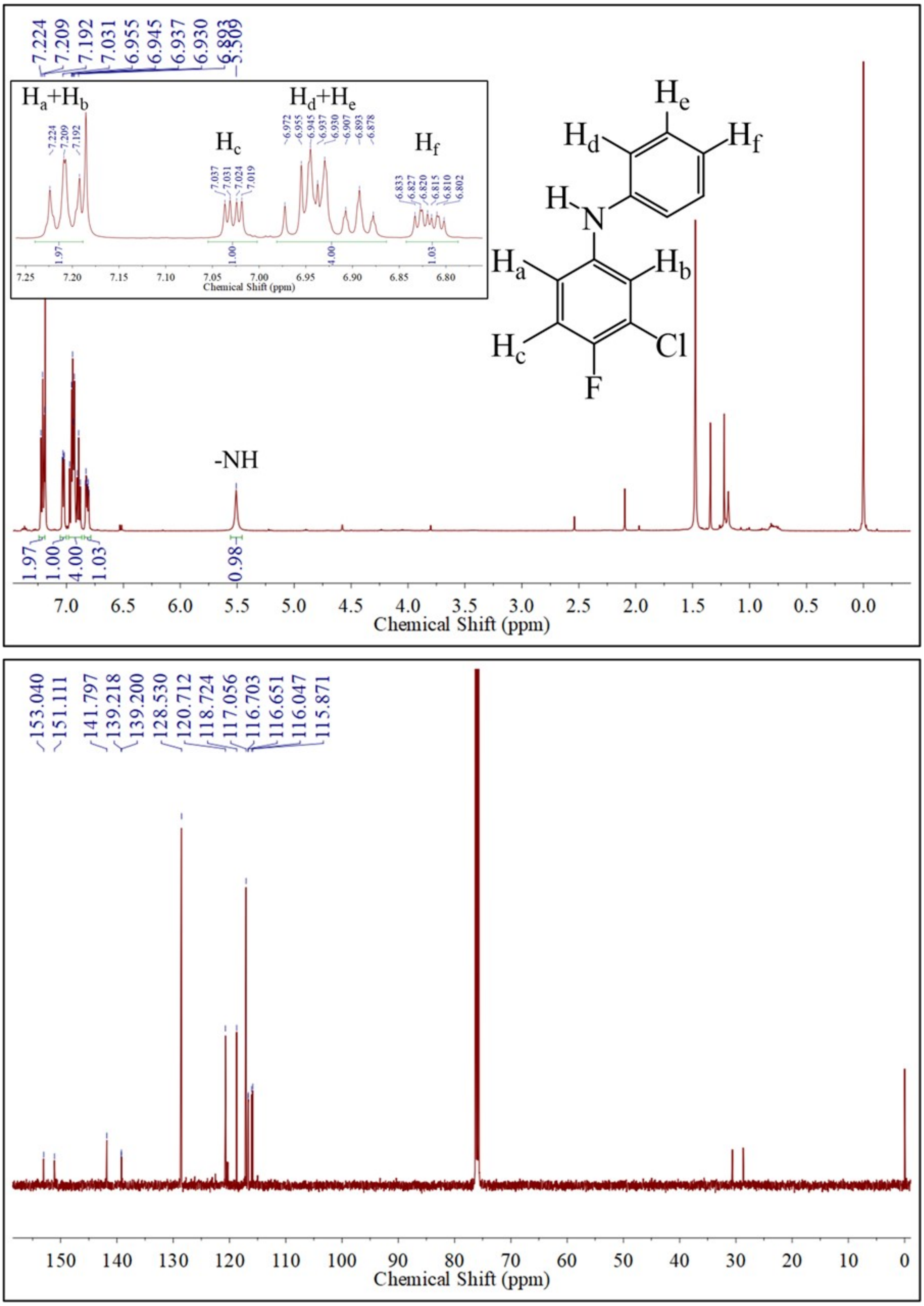


**Figure S22.** (a) $^{1}H$ NMR ($CDCl_3$, 500 MHz) and (b) $^{13}C$ ($CDCl_3$, 500 MHz) of Chan-Lam coupling product of 3-chloro-4-fluoroaniline and phenylboronic acid catalyzed by **Cu-CDA-MOF.**

(a)

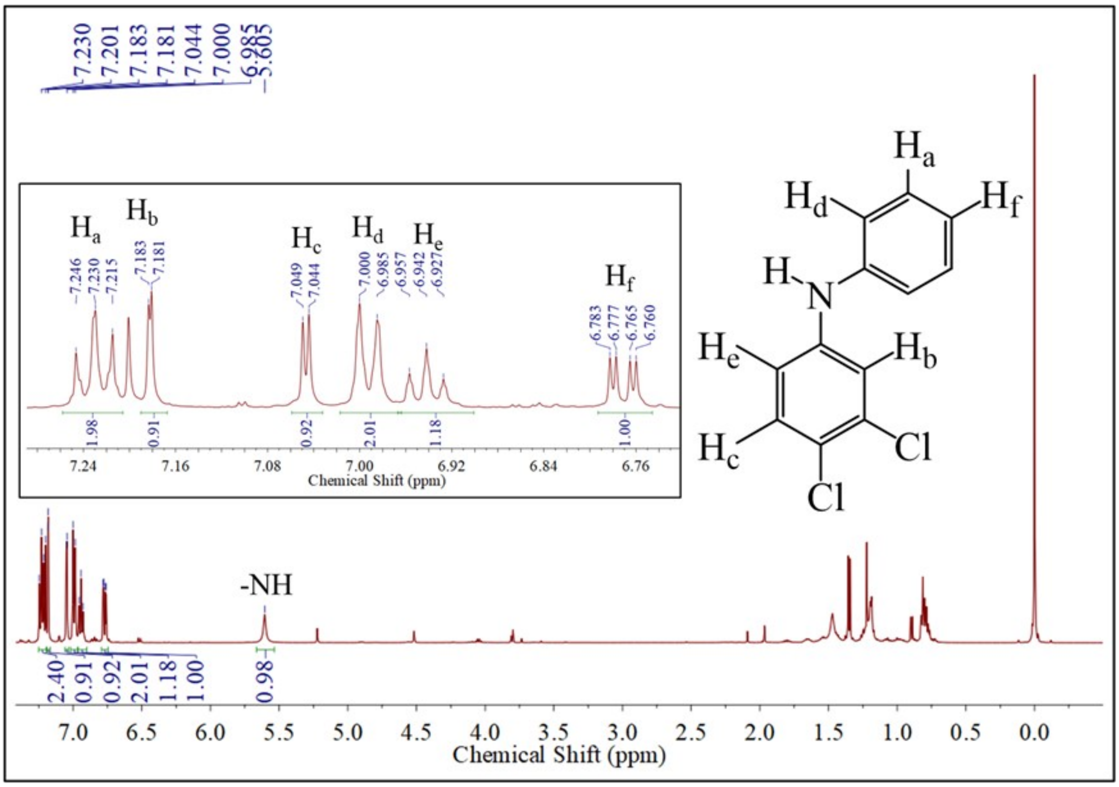


(b)

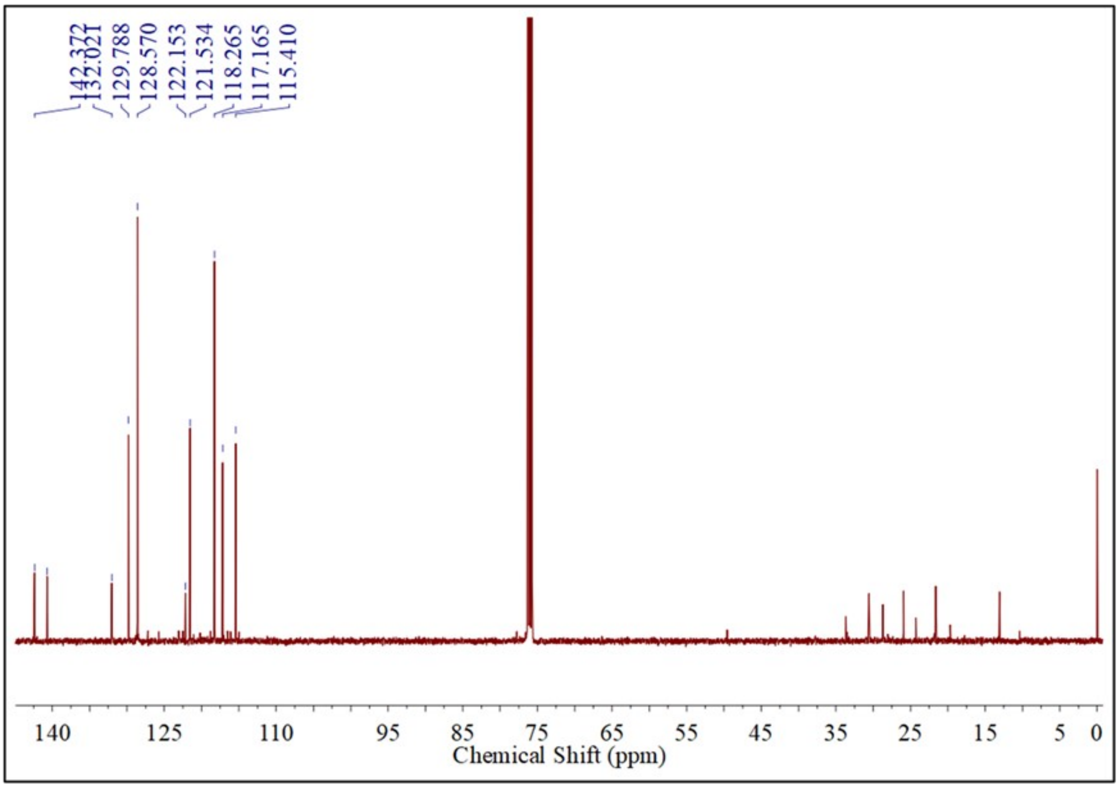


**Figure S23.** (a) $^{1}H$ NMR ($CDCl_3$, 500 MHz) and (b) $^{13}C$ ($CDCl_3$, 500 MHz) of Chan-Lam coupling product of 3,4-dicholoroaniline and phenylboronic acid catalyzed by **Cu-CDA-MOF.**

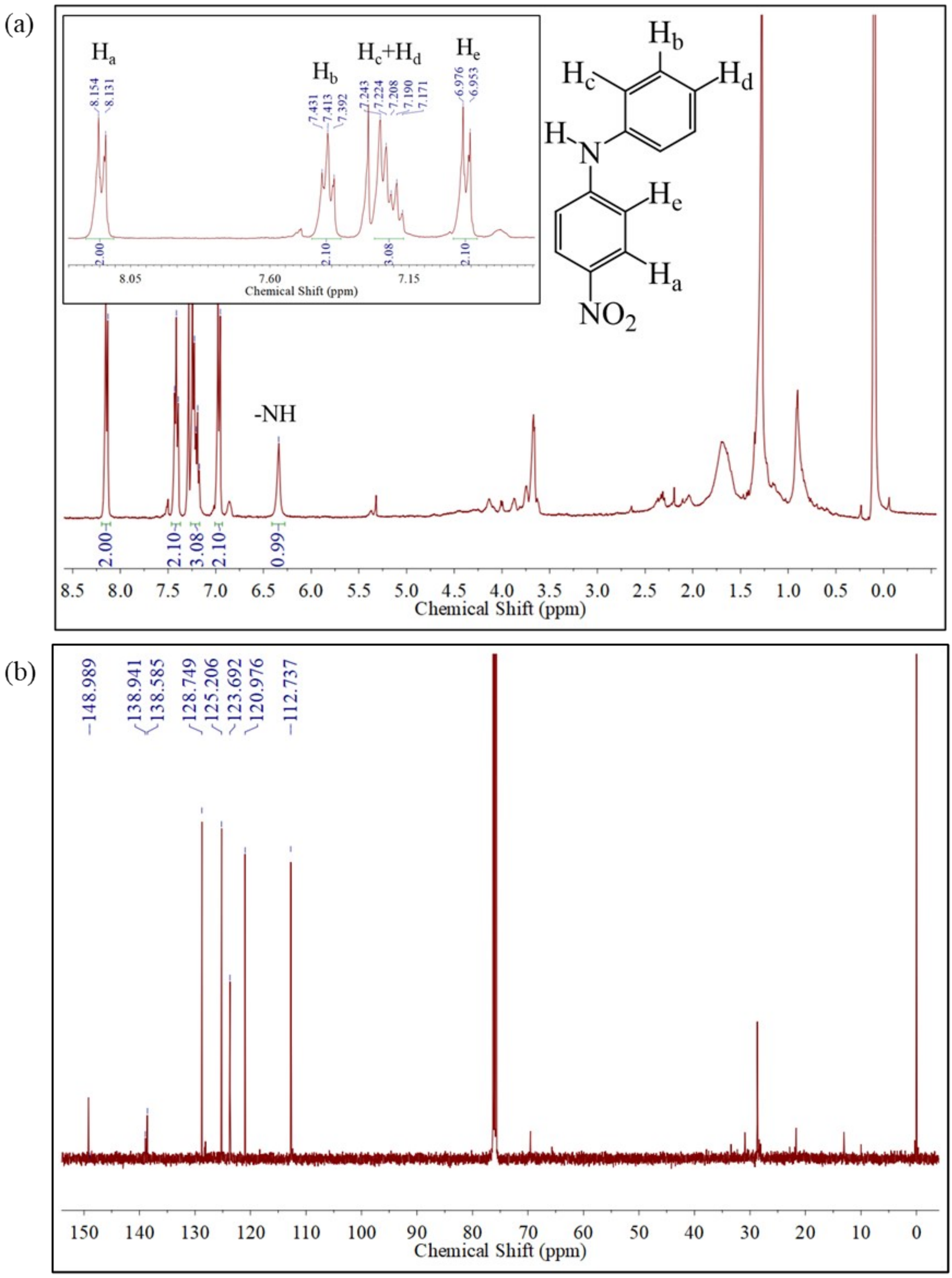


**Figure S24.** (a) $^{1}H$ NMR ($CDCl_3$, 400 MHz) and (b) $^{13}C$ ($CDCl_3$, 500 MHz) of Chan-Lam coupling product of 4-nitroaniline and phenylboronic acid catalyzed by **Cu-CDA-MOF.**

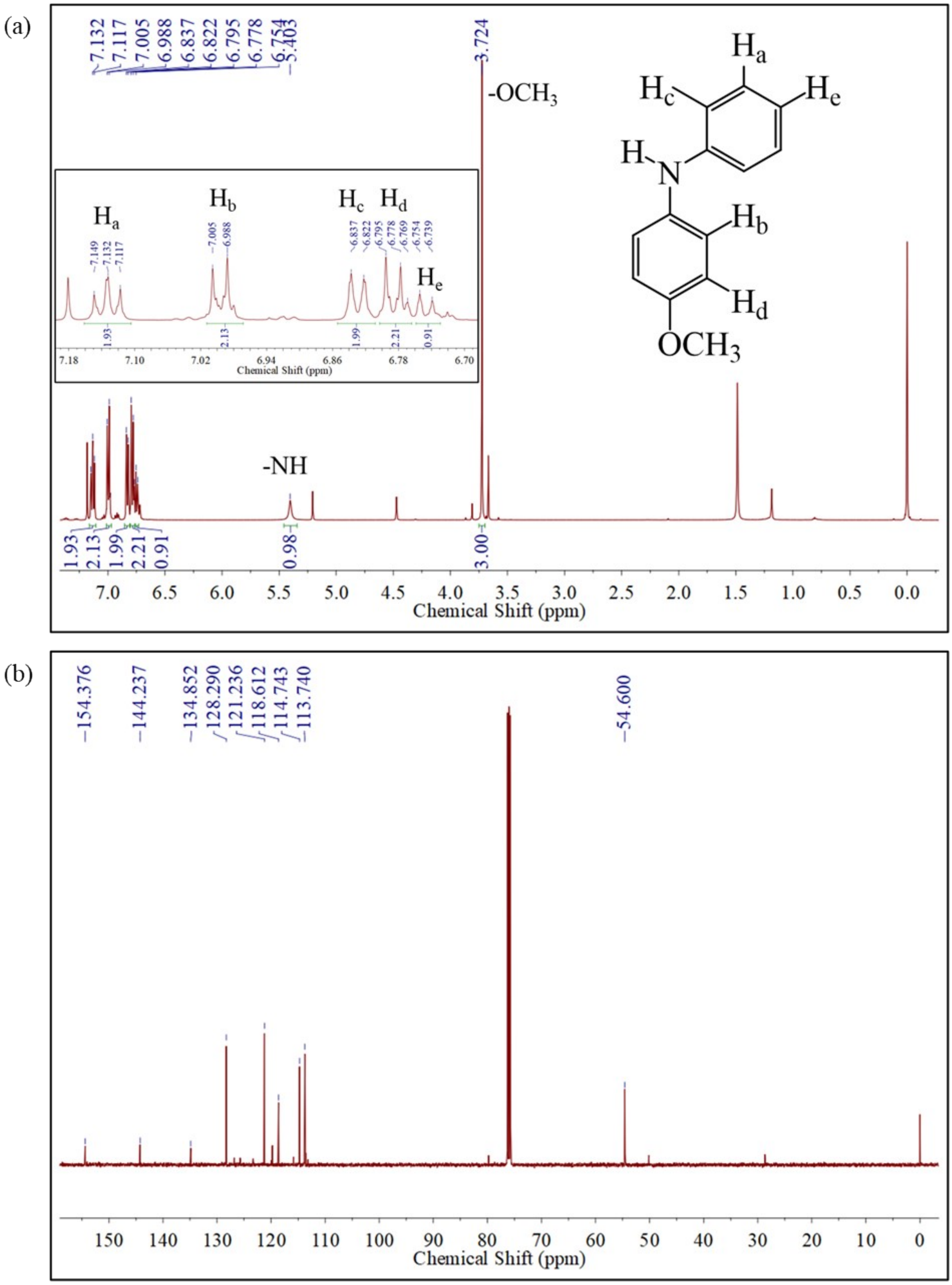


**Figure S25.** (a) $^{1}H$ NMR ($CDCl_3$, 500 MHz) and (b) $^{13}C$ ($CDCl_3$, 500 MHz) of Chan-Lam coupling product of 4-methoxyaniline and phenylboronic acid catalyzed by **Cu-CDA-MOF.**

**<u>Section S8</u>:** Comparison Table for Catalytic Activity and Conversion Efficiency of **Cd-CDA-MOF** and **Cu-CDA-MOF** with the recently reported MOF catalysts

**Table S3.** Comparison table of Catalytic Activity and Conversion Efficiency of **Cd-CDA-MOF** towards Knoevenagel Condensation Reaction

| **MOFs** | **Temp. (˚ C)** | **Yield (%)** | **TON** | **TOF ($h^{-1}$)** | **References** |
|---|---|---|---|---|---|
| **Ni-MOF** nanosheets | RT | 99 % | - | - | *Nano Res.*, **2019**, *12*, 437 |
| **TMU-41** | RT | 98 % | - | - | *Polyhedron*, **2019**, *159*, 72. |
| **V-Zn-MOF** | 60 ˚C | 99 % | - | - | *ACS Sustainable Chem. Eng.*, **2021**, *9*, 4660. |
| **Zn-MOF** | 60 ˚C | 99 % | - | 167 | *Inorg. Chem.* **2018**, *57*, 11157 |
| **Cd-PBA** | RT | 91 % | - | - | *Cryst. Growth Des.***2018**, *18*, 2883. |
| [Cd(4-btapa)$_2$(NO$_3$)$_2$]·6H$_2$O·2DMF | RT | 98 % | - | - | *J. Am. Chem. Soc.*, **2007**, *129*, p. 2607. |
| **CAU-1-NH$_2$** | 40 ˚C | 94 % | - | - | Cryst Eng Comm, **2017**, *19*, 4187. |
| **Cd-CDA-MOF** | RT | >99 | 182.49 | 15.21 | This work |

**Table S4.** Comparison table of Catalytic Activity and Conversion Efficiency of **Cu-CDA-MOF** towards Chan-Lam Coupling Reaction

| **MOFs** | **Temp. (˚ C)** | **Isolated Yield (%)** | **TOF ($h^{-1}$)** | **References** |
|---|---|---|---|---|
| **$Cu_2(BDC)_2(BPY)$-MOF** | RT | 85 % | - | *RSC Adv.*, **2017**, *7*, 46022. |
| **Cu-MOF {[$Cu(4\text{-}tba)_2$](solvent)}$_n$** | 40˚ C | 98 % | - | *Inorg. Chem. Commun* **2015**, *61*, 13. |
| **Cu(tpa)-MOF** | RT | 76 % | - | *Chem Cat Chem.*, **2016**, *8*, 2953. |
| **URJC-1-MOF** | 60˚ C | 79 % | - | *Chem Cat Chem.*, **2019**, *11*, 3376. |
| **Cu(II)-complexes** | RT | 64 % | - | *Chem Cat Chem.*, **2020**, *12*, 3010 |
| **Cu-CDA-MOF** | 60˚ C | 70 % | 350 | This work. |